Proceedings of the I·R·E

NOVEMBER 1942

VOLUME 30 NUMBER 11

Institute of Radio Engineers

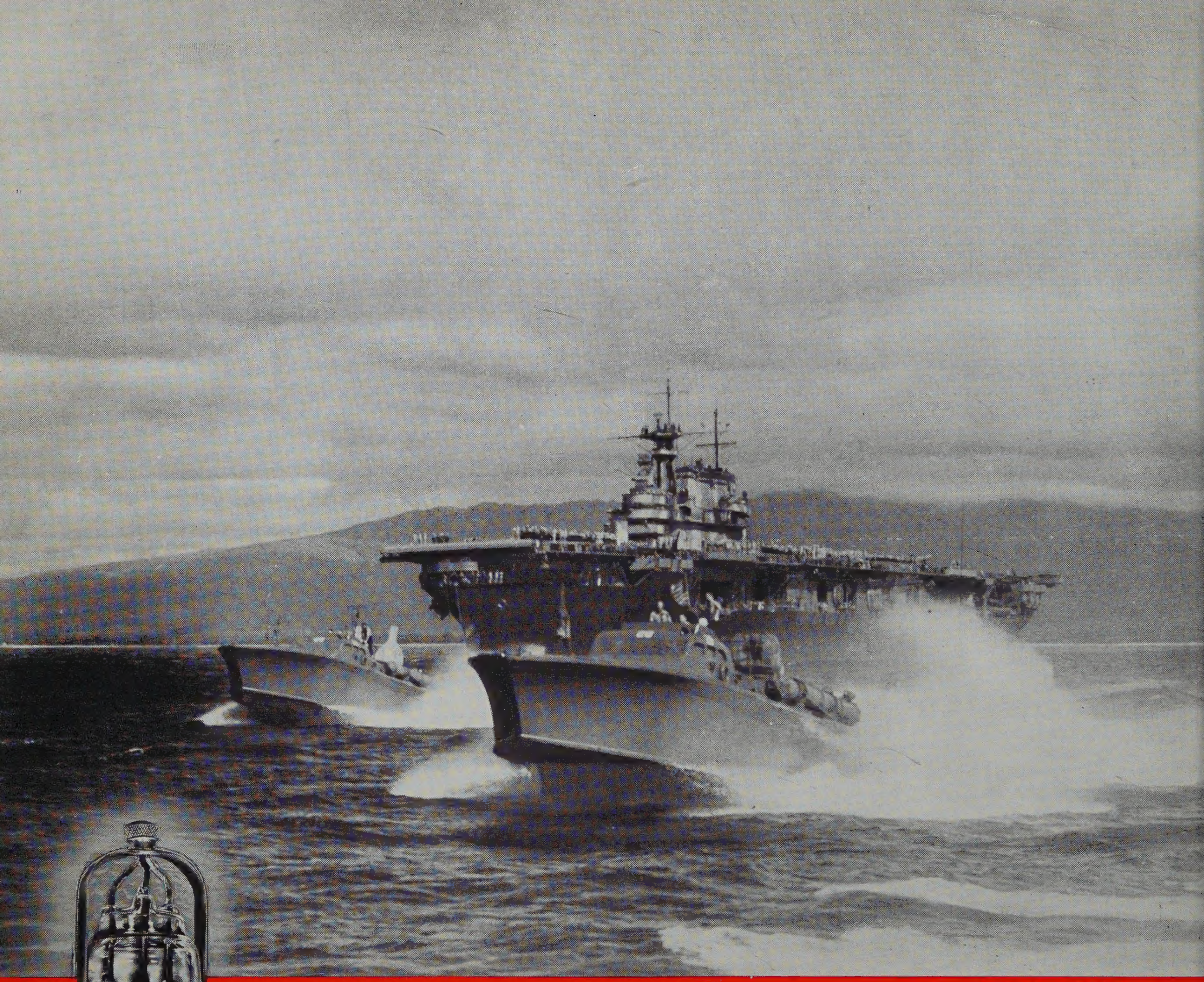

U. S. Navy Official Photo

Proceedings of the I·R·E

Published Monthly by
The Institute of Radio Engineers, Inc.

VOLUME 30 — *November, 1942* — NUMBER 11

The contents of papers published in the PROCEEDINGS are the responsibilities of the authors and are not binding on the Institute or its members.

Entered as second-class matter October 26, 1927, at the post office at Menasha, Wisconsin, under the Act of February 28, 1925, embodied in Paragraph 4, Section 538 of the Postal Laws and Regulations. Publication office, 450 Ahnaip Street, Menasha, Wisconsin. Editorial and advertising offices, 330 West 42nd St., New York, N. Y. Subscription $10.00 per year; foreign, $11.00.

THE INSTITUTE OF RADIO ENGINEERS
INCORPORATED

New York Meeting—December 2, 1942

SECTION MEETINGS

ATLANTA November 20	CHICAGO December 18	CLEVELAND November 26	DETROIT November 20
LOS ANGELES November 17	PHILADELPHIA December 3	PITTSBURGH December 14	WASHINGTON December 14

SECTIONS

ATLANTA—Chairman, J. M. Comer; Secretary, M. H. Honnell, Elec. Eng. Dept., Georgia School of Technology, Atlanta, Ga.

BALTIMORE—Chairman, G. J. Gross; Secretary, A. D. Williams, Bendix Radio Corp., E. Joppa Rd., Towson, Md.

BOSTON—Chairman, R. F. Field; Secretary, R. O. Oberg, Northeastern Univ., Boston, Mass.

BUENOS AIRES—Chairman, J. P. Arnaud; Secretary, Alexander Nadosy, Florida St. 1065, Dept. C-6, Buenos Aires, Argentina.

BUFFALO-NIAGARA—Chairman, F. H. Scheer; Secretary, A. J. Dybowski, Dymac Radio, Inc., 1531 Main St., Buffalo, N. Y.

CHICAGO—Chairman, R. A. Kay; Secretary, Walter Kenworth, 5505 Potomac Ave., Chicago, Ill.

CINCINNATI—Chairman, W. L. Schwesinger; Secretary, Howard Leppele, 4432 Raceview Ave., Cincinnati, Ohio.

CLEVELAND—Chairman, P. L. Hoover; Secretary, A. S. Nace, 3209 Archwood Ave., Cleveland, Ohio.

CONNECTICUT VALLEY—Chairman, W. M. Smith; Secretary, R. E. Moe, Radio Dept., General Electric Co., Bridgeport, Conn.

DALLAS-FORT WORTH—Chairman, Truett Kimzey; Secretary, P. C. Barnes, Radio Station WFAA-WBAP, Grapevine, Texas.

DETROIT—Chairman, H. F. Tank; Secretary, E. J. Hughes, 14209 Prevost, Detroit, Mich.

EMPORIUM—Chairman, R. K. Gessford; Secretary, H. D. Johnson, Hygrade Sylvania Corp., Emporium, Pa.

INDIANAPOLIS—Chairman, S. E. Benson; Secretary, B. H. Rinehart, 1920 Park Ave., Indianapolis, Ind.

KANSAS CITY—Chairman, H. K. Morgan; Secretary G. L. Taylor, Midland Radio School Power and Light Building, Kansas City, Mo.

LOS ANGELES—Chairman, C. F. Wolcott; Secretary, E. S. Sievers, Room 567, 417 S. Hill St., Los Angeles, Calif.

MONTREAL—Chairman, J. A. Ouimet; Secretary, J. R. Bain, Dept. 912, Northern Electric Co., 1231 Shearer St., Monteal, Que., Canada.

PHILADELPHIA—Chairman, J. B. Coleman; Secretary, H. J. Schrader, Bldg. 8, Fl. 10, RCA Manufacturing Co., Camden, N. J.

PITTSBURGH—Chairman, D. A. Myer; Secretary, A. P. Sunnergren, West Penn Power Co., 14 Wood St., Pittsburgh, Pa.

PORTLAND—Chairman, R. W. Deardorff; Secretary, B. R. Paul, 5960 S. W. 41st. Ave., Portland, Ore.

ROCHESTER—Chairman, O. L. Angevine, Jr.; Secretary, G. R. Town, Stromberg-Carlson Tel. Mfg. Co., Rochester, N. Y.

ST. LOUIS—Chairman, O. S. McDaniel; Secretary, H. D. Seielstad, 1017 S. Berry Rd., St. Louis, Mo.

SAN FRANCISCO—Chairman, H. E. Held; Secretary, W. G. Wagener, Heintz and Kaufman, South San Francisco, Calif.

SEATTLE—Chairman, K. H. Ellerbeck; Secretary, H. E. Renfro, 4311 Thackeray Pl., Seattle, Wash.

TORONTO—Chairman, T. S. Farley; Secretary, L. C. Simmonds, A. C. Simmonds and Sons, 301 King St., E., Toronto, Ont., Canada.

TWIN CITIES—Chairman, R. E. Allison; Secretary, A. G. Peck, Twin-Cities Studios, Columbia Broadcasting System, 625 Second Ave., S., Minneapolis, Minn.

WASHINGTON—Chairman, E. M. Webster; Secretary, J. D. Wallace, Radio Division U. S. Naval Research Laboratory, Anacostia Station, D. C.

Proposed Standard Conventions for Expressing the Elastic and Piezoelectric Properties of Right and Left Quartz*

W. G. CADY†, FELLOW, I.R.E., AND K. S. VAN DYKE†, MEMBER, I.R.E.

Summary—*Three sources of confusion in the literature on quartz crystals have recently been pointed out:*[1] *the distinction between right and left quartz, the conventions respecting the positive directions of the crystal axes, and conventions respecting the signs of angles when the axial system is rotated. After further consideration of this subject in the present paper, it is recommended that writers employ only that definition of right and left quartz which is now generally accepted, and that uniform conventions be agreed upon for axial directions and rotations. Voigt's usage in the main is advocated with this important exception: it is proposed that a right-handed system of axes be used for right quartz, left-handed for left quartz. This arrangement may appropriately be called the Right-Left axial system. The advantages are that all elastic and piezoelectric constants then retain the same sign for both types of crystal, and that all equations having to do with rotated axes apply equally to both types. No heed need be given to the distinction between right and left quartz except when angles are to be laid off on an actual specimen, and then the difference lies only in the reversal of the x axis for left quartz. A table showing the conventions used by various authors is included.*

Introduction

THE literature on quartz crystals is in a state of great confusion, in the use of the terms "right," "left," "positive," and "negative." This confusion is of three sorts, of which the first arises from the fact that quartz crystals are *enantiomorphic;* that is, they occur in both *right* and *left* forms. Not only in the arrangement of external faces but also with respect to all physical properties one is the mirror image of the other. Not all writers are agreed as to which form should be called "right."

The second source of confusion is the lack of agreement among different authors as to the positive sense of the x and y axes, for both right and left quartz.

The third troublebreeder is found in the equations for transformation of elastic and piezoelectric constants to rotated axes: a clockwise rotation is called by some writers positive, by others negative.

Even if all writers had clearly stated all their conventions, the task of comparing and interpreting their results would be troublesome enough. The too-frequent lack of such statements has brought the situation to an intolerable state. For this confusion Voigt[2] himself is partly responsible. If he could have foreseen the development of the electron tube and the important uses to which, in conjunction with electron tubes, piezoelectric crystals, and especially quartz, were destined to be put, he would doubtless have assembled at one point his system of conventions, instead of leaving them scattered casually throughout the pages of the *Lehrbuch*, where they have escaped the attention of most investigators. Indeed, even he uses in the *Lehrbuch* a definition of signs of angles of rotation differing from that in some of his earlier publications.

The two forms of quartz can be distinguished by the disposition of certain faces, when those faces happen to be present (see below). Another method in common use, which can be applied to any specimen, whether natural faces are present or not, takes advantage of the fact that quartz crystals are also *optically active.* When a beam of plane-polarized light passes through the crystal parallel to the optic (z) axis, the plane of polarization becomes progressively rotated, and the direction of rotation is opposite in right quartz from that in left. Confusion has arisen from the fact that a beam of polarized light is rotated to the right or left (clockwise or counterclockwise) according to whether or not the gaze of the observer is in the direction of propagation of the beam. This subject is well discussed by Sosman[3] and more recently by Van Dyke,[1] who points out that while most leading authorities today call the rotation "right" or "positive" when it appears clockwise to an observer looking back at the light source (that is, in a direction contrary to that of the beam), the opposite convention has been employed by some.

Fortunately the crystallographers are in agreement in calling α quartz *right* when the "*sx*" combination of faces, on a crystal held with its optic axis vertical and with a face of the primary positive first-order rhombohedron (an r face) at the *upper front*, appears at both ends of that prismatic edge which is at the *right* of this r face (Fig. 1). This definition is purely a matter of convention. What is not a convention but a fact is that in a crystal satisfying this definition of "right" a beam of plane-polarized light parallel to the optic axis becomes rotated to the *left* from the point of view of the *source of light.* Nevertheless, if we adopt the convention that the direction of rotation is that

* Decimal classification 537.65. Original manuscript received by the Institute, August 19, 1940; revised manuscript received, September 8, 1942. The question of terminology has been raised independently by W. P. Mason and G. W. Willard, "Piezoelectric Crystals," Proc. I.R.E., vol. 28, p. 428; September, 1940, with the suggestion that a committee of the Institute be appointed to recommend a standardization of quartz terminology. The Board of Directors appointed such a committee consisting of K. S. Van Dyke (chairman); J. D. Crawford (secretary); C. F. Baldwin, S. A. Bokovoy, W. L. Bond, W. G. Cady, J. K. Clapp, and W. P. Mason. The definitions and conventions as set forth in the present paper have received the approval of this committee and will be included in its final report.

† Wesleyan University, Middletown, Connecticut.

[1] Karl S. Van Dyke, "On the right- and left-handedness of quartz and its relation to elastic and other properties," Proc. I.R.E., vol. 28, pp. 399–406; September, 1940.

[2] W. Voigt, "Lehrbuch der Kristallphysik," Teubner, Leipzig, Germany, 1910, also second edition, 1928.

[3] R. B. Sosman, "The Properties of Silica," Chemical Catalog Company, New York, 1927, p. 856.

seen by an observer looking back *toward the source,* a given crystal is either "right" or "left" from both the crystallographic and the optical standpoints. Although this convention, used also by Voigt, has become generally recognized as standard, examples of the opposite

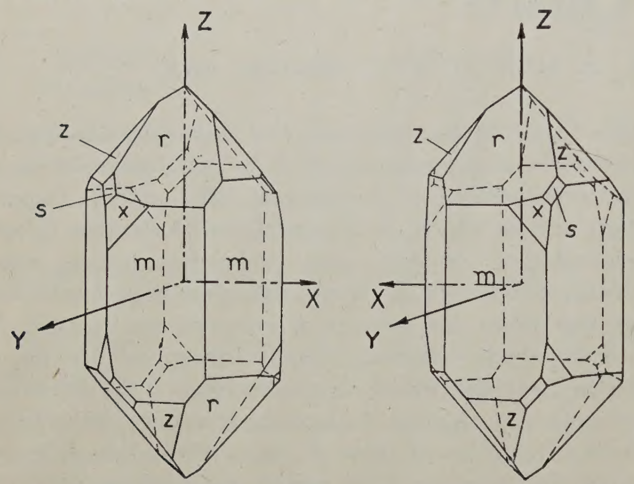

Fig. 1—Left and right quartz crystals, showing the positive directions of axes as recommended in this paper.

and obsolescent terminology can be found, without accompanying explanations, in recent papers.

This paper is a plea for consistency, and it advocates a system of conventions containing only one important departure from the usage of Voigt's *Lehrbuch*, which, if generally adopted, should remove all confusion and ambiguity. While these recommendations have to do explicitly only with quartz, they are applicable in principle to all enantiomorphic crystals, that is, all crystals that occur in both right and left types.

Faces and Axes of Right and Left Quartz

At the risk of repeating much that is already familiar to the reader, it seems desirable to summarize briefly those characteristics of quartz crystals that concern us here. The most prominent faces of a quartz crystal are the prismatic m faces and the inclined faces r (the primary positive first-order rhombohedron), and z (primary first-order negative rhombohedron) at the ends of the optic or z axis as shown[4] in Fig. 1. Usually the z faces are less developed and also less smooth than the r faces. It is in terms of the r faces that the y axes are defined. If a given specimen fails to possess natural faces sufficient for sure identification of the axes, recourse must be had to tests by such means as etch figures or X rays for all axes, and polarized light for the z axis. By static piezoelectric tests nothing better than a rough approximation to the direction of the x axis can be obtained, unless very elaborate means are employed. The use of etch figures and polarized light has recently been discussed by Van Dyke.[1]

The faces that betray the right and left handedness of quartz are the s and x faces shown in Fig. 1. On many crystals no trace of these faces can be found. Although such specimens do not exhibit the enantiomorphic property externally, still their structure is as truly enantiomorphic as if the s and x faces were present.

Following is Voigt's convention[5] for the definitions of the z and y axes in both right and left quartz:

The *z axis* is the optic axis, parallel to the edges of the prism. *Either end may be called positive;* diagrams usually show the $+z$ direction pointing vertically upward in the plane of the paper.

There are three possible y axes, normal to the prismatic faces, *the positive direction of each pointing outward from a prismatic face that intersects an r face at the $+z$ end of the crystal.*[6]

Most writers, including Voigt, have employed a right-handed system of orthogonal axes for both right and left quartz. The serious disadvantage is that in passing from one type to the other the signs of all piezoelectric constants have to be changed, as well as certain signs in the equations for the transformation of axes. Fig. 1 agrees with the Voigt convention for right quartz, but for left quartz our x axis is opposed to his, as will be seen presently.

These annoyances and potential sources of error are completely avoided by the adoption of a *right-handed axial system for right quartz, left-handed for left quartz.* We shall refer to this proposed arrangement as the *Right-Left axial system.*

The advantages of such an arrangement were pointed out by Koga[7,8] as early as 1929. His recommendation, however, involves the use of x and y axes both of which are opposed to those of Voigt for right quartz. Not only does this run counter to almost everything else in the literature, but it adds to the confusion by demanding changes in sign of some, but not all, of the elastic and piezoelectric constants.

Very recently a similar proposal has been made by Mason and Willard.[9]

Therefore, we propose as the definition of the positive end of an x axis that end at which a *positive charge* appears when the *x_x strain is positive* (see definitions of strains below); this is equivalent to stating that a *negative* charge appears at the positive

[4] In conformity with current practice we designate by z the faces called by Groth and others the r' faces. The symbols z and x for *faces* must not be confused with the z and x *axes.*

[5] See page 750 of footnote reference 2.

[6] It is of course understood that the axes of a crystal are *directions* in the crystal, and not particular lines. The existence of three y axes (and three corresponding x axes) is a consequence of the trigonal symmetry of quartz crystals; in equations and diagrams it is immaterial which of the three possible directions is selected for the y axis (and for the x axis perpendicular thereto), as long as the same axes are retained throughout the discussion. When it comes to cutting a plate from a given crystal, the selection of a particular axial system out of the three possible ones will depend on such considerations as economy of material and avoidance of flaws and twinned regions.

[7] I. Koga, "Piezoelectricity and its applications," *Jour. I. E. E.* (Japan), pp. 49–92; July, 1929.

[8] I. Koga, "Comments on the National Physical Laboratory's notation for piezoelectric quartz," *Electroteck. Jour.* (Japan), vol. 2, pp. 287–289; December, 1938.

[9] W. P. Mason, and G. W. Willard, "Piezoelectric crystals," Proc. I.R.E., vol. 28, p. 428, September, 1940.

end of an x axis upon *compression* along this axis. If the original crystal has identifiable x or s faces, the positive end of an x axis as thus defined can be determined at once, since it always emerges at a prismatic edge where the x and s faces are found. According to the present proposal these statements become valid for both right and left quartz.

The x axis defined in this manner is shown in Fig. 1. Unless otherwise stated this definition of the x axis is employed throughout the remainder of the present paper. It is evident that the right- or left-handedness of the axial system is the same as that of the crystal itself. In other words, according to the Right-Left system, in left quartz both the geometrical form and the system of reference axes are the mirror images of those for right quartz. Moreover, as has been stated, the same is true of all physical properties of the crystal.

Mirror Images

It may be helpful at this point to consider the nature of mirror images.

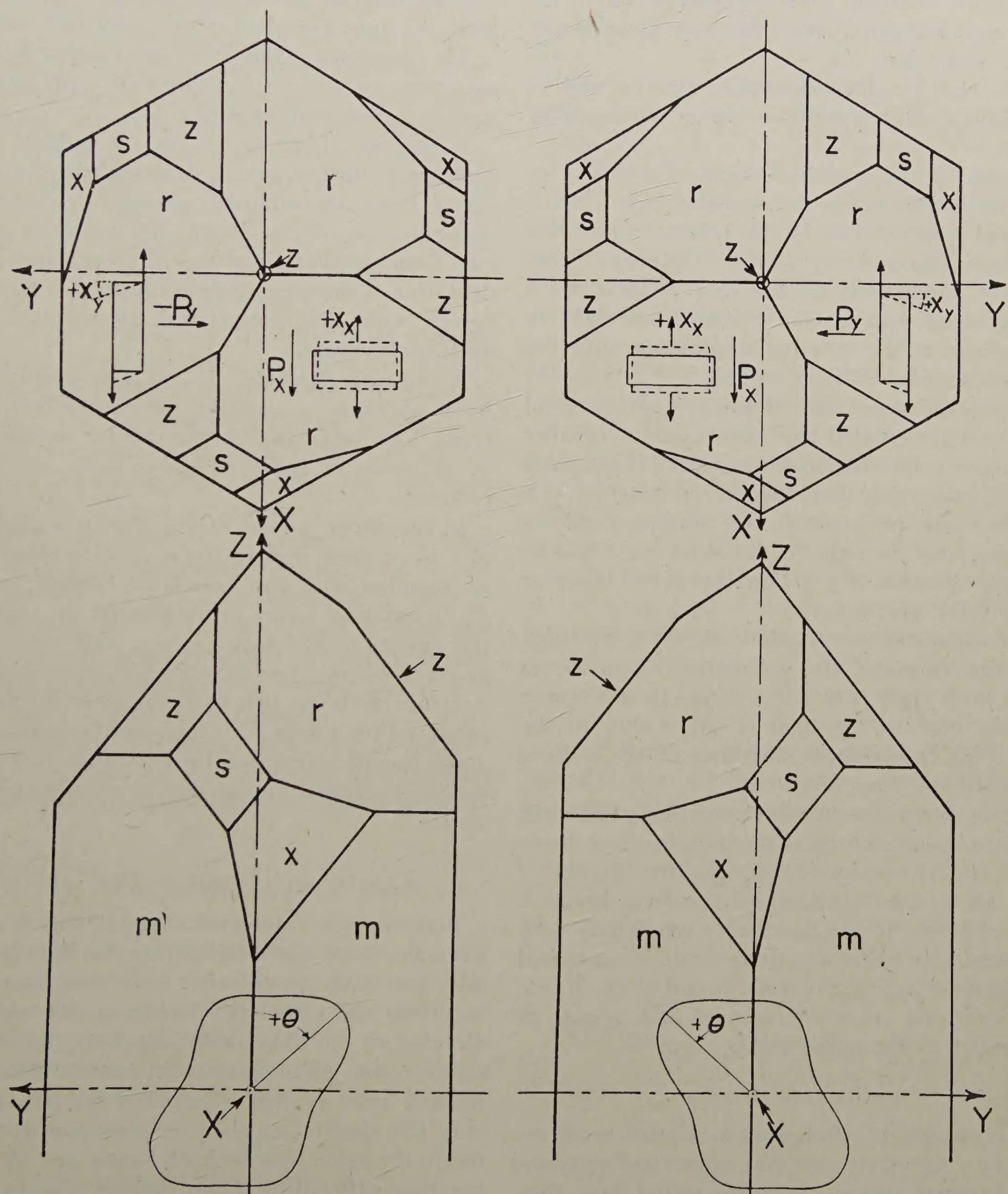

Fig. 2—Left and right quartz, showing strains $+x_x$ and $+x_y$, with accompanying polarizations P_x and P_y, also showing the positive sense of the angle of rotation θ.

When an image is formed of an object by reflection in a mirror, the orientation of the image with respect to the object, but not the form of the image, depends upon the position of the mirror. In representing right and left forms of crystals it is customary to place the

two diagrams side by side with the z axis vertical. For example, in Fig. 2 the right-hand portion is the reflection of the left with respect to a mirror whose normal is horizontal and in the plane of the paper. The advantage of this mode of reflection is that it leaves the z axis unchanged in the transition from right to left. It should be added that in Fig. 1, as in most textbooks, the line drawing of the left form, while entirely correct, does not strictly represent a mirror image of that of the right; it is as if a slight rotation has been given to the crystal after reflection.

The right and left diagrams might equally well be made with the z axis horizontal or indeed in any other orientation.

In any case, if the crystal diagram of which a reflected image is desired has incorporated in it a right-handed axial system, then in the *reflected figure* this axial system is necessarily *left handed*. The change from right to left handedness of the axes is therefore a logical accompaniment to the change from right to left handedness in the external appearance and the physical characteristics of the crystal.

If a photograph were taken of a right quartz crystal showing the right-handed xyz axial system together with all curves, polar diagrams, and models illustrating its physical properties, then the mirror image of this picture, obtained, for example, by making a photographic print with the negative turned over, would be an exact reproduction of a left quartz crystal together with its physical properties.

These considerations are made clear in Fig. 2, which shows an end view and also a cross section in the yz plane, for both right and left quartz. In the upper diagram the positive direction of the z axis, in the lower diagram the positive direction of the x axis, points toward the observer.

This figure shows also an x-cut plate being stretched so that there is an extensional strain x_x in the x direction with an accompanying contraction in the y direction. The arrow P_x indicates the positive direction of the ensuing electric polarization, in conformity with the statement above that a positive strain is associated with a positive charge at the positive end of the x axis. *Compressional and extensional strains and stresses do not change sign in the mirror image.*

Stresses and Strains

There is danger of confusion in elastic problems between the external stresses that cause elastic strains, and the internal reacting stresses called into play thereby, which, for a system in equilibrium, are equal and opposite to the former. Voigt calls *an extensile strain positive, and the internal reacting stress also positive.* This convention is analogous to the customary association of $+p$ with $+v$ in the laws of gases. It is thus that Voigt is led to regard a positive strain as due to a *negative externally applied* stress. Some well-known texts define a positive stress as that which, applied from without, causes a positive strain. In conformity with most writers on piezoelectric subjects we shall follow Voigt, whose definitions may be stated thus:

A longitudinal strain (that is, a contraction or extension in the direction of the compressional or extensional stress producing it), of type x_x, y_y, or z_z, is positive when it is an extension, negative when a contraction.

A *longitudinal stress* (X_x, Y_y, Z_z) is positive when it tends to cause a negative strain, and vice versa.

The foregoing definitions are exemplified in such equations as $x_x = -s_{11}X_x$, where the compliance coefficient s_{11} is essentially positive.

A *shearing strain* (y_z, z_x, x_y) is positive when the *acute* angle formed by the deformation of a rectangle, whose sides are originally parallel to the two axes corresponding to the shear, lies in the quadrant between the *positive* directions of these axes. The usual definition of shearing strain, of form $x_y = \partial v/\partial x + \partial u/\partial y$ agrees with this geometrical interpretation of the sense of the strain.

A *shearing stress* (Y_z, Z_x, X_y) is positive when it tends to cause a negative shearing strain, and vice versa. The compliance coefficients for shears, occurring in equations of the type $x_y = -s_{66}X_y$, are essentially positive.

In the upper portion of Fig. 2 is indicated a section of a y-cut plate undergoing a positive shearing strain x_y, together with the associated electric polarization P_y. Tangential forces are indicated by arrows. From the equation $P_y = e_{26}x_y = -e_{11}x_y$ and the sign of e_{11} as given below, it is seen that P_y is negative. In accordance with our proposal, the piezoelectric shear x_y produced by a field E_y in the positive direction of the y axis has the same sign for left as for right quartz. A similar statement applies also to all other piezoelectric shears.

Elastic and Piezoelectric Constants

According to Voigt's notation, all elastic coefficients have the same signs for left as for right quartz, but the signs of all piezoelectric constants change in passing from right to left. Attention has already been directed to the changes in sign that this demands in elastic and piezoelectric equations. When a left-handed axial system is adopted for left quartz, not only the elastic but also the piezoelectric coefficients retain the same sign for both forms, and all equations, together with all direction cosines, remain absolutely unaltered. Not until the time comes for laying off angles on an actual specimen is it necessary to pay any attention to the question of right or left handedness, and then all that must be remembered is to use left-handed axes for left quartz, in accordance with Figs. 1 and 2.

Voigt assigns negative numerical values to the constants d_{11}, e_{11}, and e_{14} for left quartz, and a positive

value to d_{14}. These signs are with respect to a right-handed axial system for left quartz. While other observers have obtained values differing in magnitude from Voigt's, there has been no disagreement as to sign. For right quartz the signs, according to Voigt, are reversed, namely, $\delta_{11}+$, $e_{11}+$, $e_{14}+$, $d_{14}-$. We advocate the adoption for the signs of the piezoelectric constants those that Voigt assigns to *right* quartz, although they are opposite to those commonly found in the literature, where in most cases the distinction between right and left quartz has not been properly taken into account. Voigt's statement that his observations were made on left quartz is so inconspicuous[10] as to be easily overlooked, and those who later made determinations seem to have been more interested in numerical magnitudes than in signs. If our suggestion is adopted, along with the Right-Left axial system, these signs will hold for *left as well as for right quartz.*

Rotated Axes

The last of our recommendations has to do with the signs of angles for rotated axes. Here it is desirable to adhere to Voigt's notation, modified for left quartz in such a way that the equations in the *Lehrbuch* for axial transformations can be used as they stand, for either right- or left-handed crystals. The proposed convention is as follows:

The angle of rotation is to be called positive when the sense of rotation is from $+x$ to $+y$, from $+y$ to $+z$, or from $+z$ to $+x$. The same rule applies to transformed axes, and on the Right-Left system it is valid for both right and left quartz. According to this rule, for *right* quartz the rotation of any pair of axes (including axes, usually designated by x' etc., that have resulted from a previous rotation), is positive when *counterclockwise* as seen from the positive end of the third axis. For *left* quartz the rotation is clockwise.

As an illustration of the rule for rotated axes there are shown in Fig. 2 polar diagrams of the distribution of Young's modulus in the yz plane. This quantity is the reciprocal of the compliance coefficient s'_{33} obtained by rotating the y and z axes through various angles θ about the x axis.[11] The maximum value is in the direction approximately perpendicular to a z face, and the corresponding angle θ, according to the Right-Left system, is approximately $+48$ degrees for both right and left quartz.

Comparison of Conventions

In conclusion, we present a tabular summary of the conventions adopted by various writers on the properties of quartz crystals.[2,12–18] Our own recommendations are included. Each author seems to have been self-consistent in the use of his own conventions.

TABLE I

Author	Convention for type of quartz		Direction of y axis		Axial system		Sign of θ for counterclockwise rotation		Location of + charge on stretch	
	l	r	l	r	l	r	l	r	l	r
Bechmann	l	r	+	+	R	R	(−)	−	−	+
Koga	l	r	−	−	R	R	−	−	+	−
Mason	r	l	(+)	(+)	(R)	(L)	−	+	−	−
Scheibe	l	r	+	+	R	R	−	−	−	+
Straubel	l	r	+	+	R	R	−	−	−	+
Voigt	l	r	+	+	R	R	+	+	−	+
Wright and Stuart	l	r	(−)	(+)	R	R	−	+	+	+
Present Recommendation	l	r	+	+	L	R	−	+	+	+

The letters l and r at the top of each column refer to the type of quartz, as defined in this paper. The first column indicates whether or not this definition was used by each writer. The second column shows the convention adopted for the positive direction of the y axis: a positive sign means agreement with Voigt's definition given above. In column 3 the letters r and l indicate whether a right- or left-handed axial system was used. The fourth column indicates the sign of the angle θ of rotation of the transformed z' axis from the z axis, for a counter-clockwise rotation in the yz plane about the x axis, as seen from the point of view of the positive side of the x axis as defined by the author quoted. The last column shows whether, with respect to the axial system adopted by the author quoted, the positive charge caused by a positive strain (stretch) parallel to an x axis would be found at the positive or negative end of this axis. Symbols are placed in parentheses when the only evidence for their correctness is inferred from equations or curves. It will be noted that the idea of a Right-Left system of axes appears implicitly in Mason's paper.

[10] See page 861 of footnote reference 2.

[11] Polar diagrams of the compliance coefficient s_{33}' itself are shown in Fig. 2 of footnote reference 1, where, although it is not so stated, the axes shown are those of the Right-Left system.

[12] R. Bechmann, "Temperature coefficients of vibrations of quartz plates and bars," *Hochfrequenz. und Elektroakustik*, vol. 44, pp. 145–160; November, 1934.

[13] I. Koga, "Notes on piezoelectric quartz crystals," Proc. I.R.E., vol. 24, pp. 510–531; March, 1936. (In this paper, Koga does not employ the convention that he advocates in his footnote reference 7.)

[14] W. P. Mason, "Electrical wave filters employing quartz crystals as elements," *Bell. Sys. Tech. Jour.*, vol. 13, pp. 405–453; July, 1934.

[15] W. P. Mason, "Low temperature coefficient quartz crystals," *Bell Sys. Tech. Jour.*, vol. 19, pp. 74–93; January, 1940. (The same conventions were used by F. R. Lack, G. W. Willard, and I. E. Fair, "Some improvements in quartz crystal circuit elements," *Bell Sys. Tech. Jour.*, vol. 13, pp. 453–463; July, 1934.

[16] A. Scheibe, "Piezoelektricität des Quarzes," Theodor Steinkopff, Dresden, Germany, 1938.

[17] H. Straubel, "Vibration mode and temperature coefficient of quartz oscillators," *Hochfrequenz. und Elektroakustik*, vol. 38, pp. 14–27; July, 1931.

[18] R. B. Wright and D. M. Stuart, "Some experimental studies of the vibrations of quartz plates," *Bur. Stand. Jour. Res.*, vol. 7, pp. 519–553; September, 1931. (The symbols in the table apply to these authors' data on Young's modulus. For their data on rigidity, the signs of θ in column 4 must be reversed.)

Operation of a Thyratron as a Rectifier*

L. A. WARE†, ASSOCIATE, I.R.E.

Summary—*The half-wave thyratron rectifier circuit is treated theoretically taking into account the difference between the firing potential and the tube drop during conduction. Four loads are considered ranging from a pure resistance to a pure inductance, the impedance angles being 0, 59.15, 85.6, and 90 degrees. The first three of these are checked oscillographically and good correspondences are obtained between (1) calculated average current and measured current and (2) oscillographic waveshape of current and calculated waveshape. It is also noted that errors in the current calculation due to erroneous values of E_f (firing potential) are higher for loads of higher impedance angles.*

AN INTERESTING digression on the general problem of rectifier analysis is the treatment of the thyratron where the firing potential differs from the tube drop during conduction. It is desirable first, to compare the calculated curve for instantaneous current with the oscillographic record; second, to find how well the calculated average current flow agrees with the measured value; and third, to calculate the effect of a change in firing potential on the average current flow. An FG-81 thyraton is considered here for four different loads, a pure resistance, two R-L circuits of different impedance angles, and a case for $R=0$. The last was calculated only.

In Fig. 1 is shown the elementary half-wave rectifier to which the following analysis may be applied.[1,2] The circuit is made up of an R-L load and a thyratron

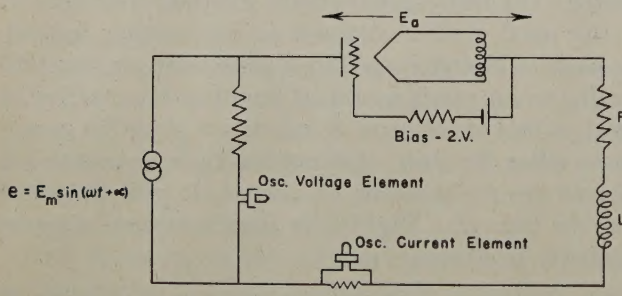

Fig. 1—Arrangement of circuit elements for obtaining oscillographic records.

which has a firing potential E_f and an assumed constant drop during conduction, E_a. Let $\alpha = \sin^{-1} E_f/E_m$ so that time may be counted from the instant of firing. The differential equation may be written

$$E_m \sin(\omega t + \alpha) - E_a = Ri + L\,di/dt. \qquad (1)$$

The solution of this equation can be written as the sum of three components

(1) the transient term $\quad i_t = I_0 e^{-Rt/L}$

(2) the constant term $\quad i_c = -E_a/R$

and (3) the alternating-current term

$$i_a = (E_m/Z)\sin(\omega t + \alpha - \theta)$$

where $Z = \sqrt{R^2 + X^2}$, and $\theta = \tan^{-1} X/R$.

$$\begin{aligned} i &= i_t + i_c + i_a \\ &= (E_m/Z)\sin(\omega t + \alpha - \theta) - E_a/R + I_0 e^{-Rt/L}. \qquad (2) \end{aligned}$$

For the determination of I_0 the boundary condition, $i=0$ when $t=0$, may be used. Thus

$$0 = (E_m/Z)\sin(\alpha - \theta) - E_a/R + I_0$$

and $I_0 = E_a/R - (E_m/Z)\sin(\alpha - \theta)$ and (2) becomes

$$\begin{aligned} i = (E_m/Z)&\sin(\omega t + \alpha - \theta) - E_a/R \\ &- [(E_m/Z)\sin(\alpha - \theta) - E_a/R]e^{-Rt/L}. \qquad (3) \end{aligned}$$

If this expression be integrated from $\omega t = 0$ to $\omega t = \phi$, the cutoff angle, and then divided by 2π, the average current is obtained. This equation is

$$\begin{aligned} I_{av} = (E_m/2\pi Z)\{&\cos(\alpha-\theta) - \cos(\phi+\alpha-\theta) - E_a\phi Z/E_m R \\ &+ (X/R)[E_a Z/E_m R - \sin(\alpha-\theta)](1 - e^{-R\phi/X})\}. \qquad (4) \end{aligned}$$

The angle of cutoff ϕ is not always easily calculated. In Section I below it is the result of direct calculation. In Sections II, III, and IV it was determined by trial from (3).

The cases which we wish to consider follow.

I. Pure Resistance Load

In this case L is set equal to zero and there immediately results

$$i = (E_m/R)[\sin(\omega t + \alpha) - E_a/E_m]. \qquad (5)$$

At the time $t=0$ this reduces to

$$i_0 = (E_m/R)(\sin \alpha - E_a/E_m).$$

However, $\alpha = \sin^{-1} E_f/E_m$ and i_0 reduces to $(E_f - E_a)/R$ which is of course to be expected at the firing point. Further, when E_f and E_a are equal we have $i_0 = 0$ at the beginning of the positive voltage loop and the case is of the usual high-vacuum tube or the large rectifier which has a relatively small firing potential.

The angle of cutoff may be found by setting the right-hand side of (5), or of (3), equal to zero. This gives

$$\sin(\phi + \alpha) = E_a/E_m$$

or ϕ, the angle of cutoff,

$$= \sin^{-1} E_a/E_m - \sin^{-1} E_f/E_m. \qquad (6)$$

The equation for the average current flow becomes, in this case,

$$I_{av} = (E_m/2\pi R)[\cos\alpha - \cos(\phi + \alpha) - E_a\phi/E_m]. \qquad (7)$$

* Decimal classification: R134×R337. Original manuscript received by the Institute, December 22, 1941.

† Department of Electrical Engineering, State University of Iowa, Iowa City, Iowa.

[1] C. M. Wallis, "Half-wave gas rectifier circuits," *Electronics*, vol. 11, pp. 12–14; October, 1938.

[2] C. M. Wallis, "Full-wave rectifier analysis," *Electronics*, vol 13, pp. 19–22; March, 1940.

In Fig. 2 is shown an oscillogram for a pure resistance load where the constants were as follows:

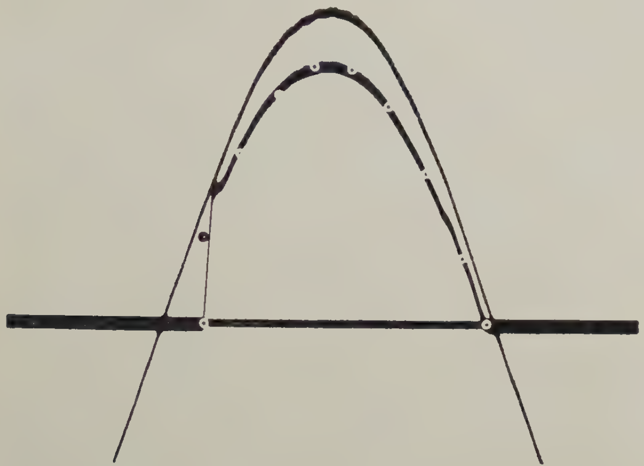

Fig. 2—Oscillogram for a pure resistance load. The small circles indicate the calculated points for the current wave. The upper curve is applied voltage.

$E_m = 164.9$ volts, $R = 137$ ohms, $E_a = 10.5$ volts, $E_f = 62.7$ volts, $\phi = 153.9$ degrees, $\alpha = 22.7$ degrees, I_{av}(measured) $= 0.321$ ampere.

E_a was determined by averaging the tube drop for several different values of current. E_f is the measured ordinate to the voltage curve at the firing point. The oscillogram shows the voltage and current waves over the conduction period and except for the portion of the current curve near to the firing point, may be considered as representing these variables sufficiently well. The calculated curve for current is represented by the points as shown. The calculated average current obtained by using the constants above was found to be 0.336 ampere, which represents a discrepancy of 4.7 per cent. It is of interest to determine the effect of a change in E_f, and for the various cases calculations will be made also for the arbitrarily chosen value of $E_f = E_a$. The calculated value of I_{av} from (7) using $E_f = E_a = 10.5$ volts gives 0.346 ampere which is within 3 per cent of the value obtained for the larger value of E_f. Table I gives I_{av} for the pure resistance case in terms of the firing potential and the firing angle.

TABLE I

α degrees	E_f volts	I_{av} ampere
3.65	10.5	0.346
10	28.6	0.345
20	56.4	0.338
30	82.5	0.327
40	106.0	0.310
50	126.3	0.288

II. $R-L$ Load. $\theta = 59.15$ Degrees

In the second case a load was used as represented by the following circuit constants. E_f was found in the same manner as above. $E_m = 164.9$ volts, $E_a = 10.5$ volts, $R = 79.5$ ohms, $X = 133.1$ ohms, $\theta = 59.15$ degrees, $\alpha = 22.4$ degrees, $E_f = 62.9$ volts, $\phi = 213.2$ degrees, I_{av}(measured) $= 0.426$ ampere.

The oscillogram of Fig. 3 shows the variation of current and voltage over the interesting range and it is noted that the cutoff angle as calculated checks reasonably well with the oscillographic record. However there is more discrepancy between the two curves at the peak than was the case in Section I.

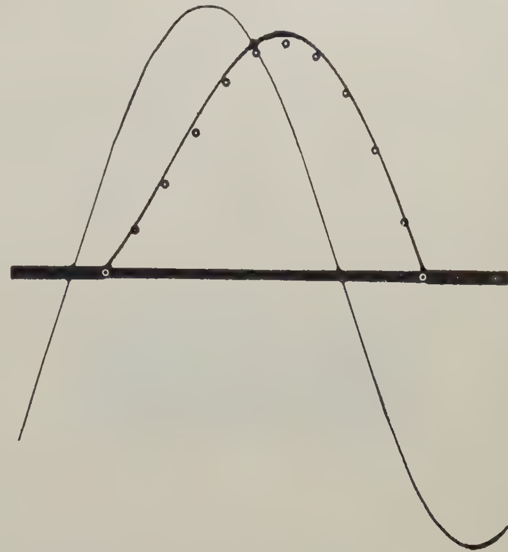

Fig. 3—Oscillogram for impedance angle of 59.15 degrees. The small circles indicate calculated points for the current wave.

The average current calculated for this case was 0.408 ampere which, compared with the measured value of 0.426, represents a discrepancy of 4.2 per cent. If E_f were equal to the tube drop of 10.5 volts, the calculated average current would be 0.423 ampere. This represents an increase of 3.7 per cent over the value for $E_f = 62.9$ volts.

It should be noted here that the conduction period is well over 180 degrees.

III. $R-L$ Load. $\theta = 85.6$ Degrees

In the case of a very small resistance component the period of conduction is still further increased as shown in Fig. 4. Here the circuit constants are: $E_m = 165$ volts, $R = 14$ ohms, $X = 182.4$ ohms, $E_a = 10.5$ volts, $E_f = 63$ volts, $\alpha = 22.7$ degrees, $\theta = 85.6$ degrees, $\phi = 264$ degrees, $I_{av} = 0.591$ ampere.

The lower set of points on this oscillogram represents the calculated current on the basis of the above constants. The agreement is seen to be somewhat good as far as the area is concerned. However the calculated angle of cutoff does not check especially well with the oscillogram. At this point it is well to mention that no account has been made of the periods of ionization and deionization of the tube. The ionization time is so short that it would not show up on the oscillogram in any case. The part of the curve belonging to the period of deionization is very small and can be neglected. The average value of current calculated for this low resistance case is 0.606 ampere, a value 2.5 per cent higher than the measured value.

Another set of points as marked represents current plotted with the above constants except that E_f is

made equal to E_a. Firing takes place earlier and cutoff later. In this case the cutoff angle is approximately

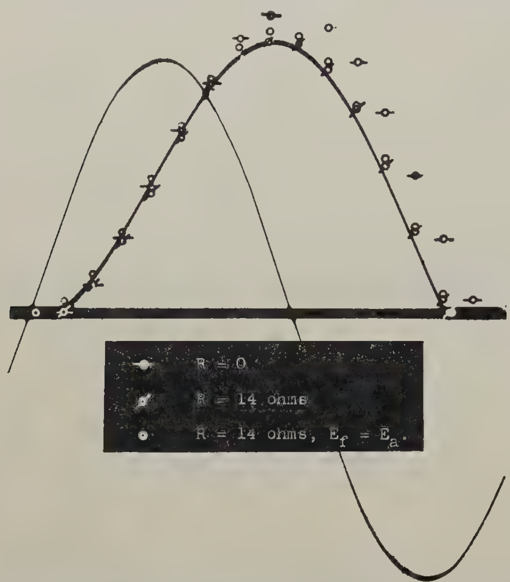

Fig. 4—Oscillogram for impedance angle of 85.6 degrees. The curves for $R=0$, $R=14$ ohms, and $R=14$ ohms with $E_f=E_a$ are plotted. The effect of the change of 14 ohms is clearly shown.

286 degrees and the calculated average current is 0.635 ampere representing an increase of 4.8 per cent over the value for the case where $E_f=63$ volts.

IV. $R=0$. $\theta=90$ Degrees

It is interesting to consider the case for $R=0$. Here we have

$$i = (E_m/X)[\cos\alpha - \cos(\omega t+\alpha) - E_a\omega t/E_m]. \qquad (8)$$

The equation for average current corresponding to this case is

$$I_{av} = (E_m/2\pi X)[\phi\cos\alpha - \sin(\phi+\alpha) + \sin\alpha - E_a\phi^2/2E_m]. \qquad (9)$$

This was calculated for the data of Section III above, assuming that $R=0$, $X=Z$, and an average value of current of 0.71 ampere was obtained, a value 20 per cent higher than for $R=14$ ohms. Due to the fact that this represented a rather unexpected increase due to a relatively small change in R the curve for $R=0$ was plotted on the oscillogram in Fig. 4 in order to see where the greatest difference occurred. It is seen that the part after the peak is moved to the right and of course the cutoff angle is greatly increased. It is impossible to check this curve oscillographically as some resistance must be present in the coil and circuit. In this case when E_f is set equal to E_a the average current is calculated to be 0.754 ampere.

In the above it is to be noted that the firing potential has been obtained from the oscillogram itself. The sources of error in the above calculations are as follows: (1) The assumption that E_a is a constant. (2) The neglect of the deionization time. (3) The assumption that the voltage wave is a sine wave. Number (1) is perhaps the most important.

Table II, in which the above calculations are summarized, presents the results of this brief investigation.

TABLE II

θ	E_f	I_{av} (meter)	I_{av} (calculated)	Per cent increase over measured value	Per cent increase over value for actual E_f
degrees	volts	ampere	ampere		
0	62.7	0.321	0.336	4.7	
0	10.5		0.346		3.0
59.15	62.9	0.426	0.408	−4.2	
59.15	10.5		0.423		3.7
85.6	63.0	0.591	0.606	2.5	
85.6	10.5		0.635		4.8
90	63.0		0.710		
90	10.5		0.754		6.2

It is seen that, in the three cases checked oscillographically, the calculated value of current was within 5 per cent of the measured value, and the variations are about the amounts to be expected upon a comparison of the oscillographic record with the calculated curves for current. It is also interesting to note that the effect of using the lower value of E_f is progressively greater for greater ratios of X to R.

The Q Meter and Its Theory*

V. V. L. RAO†, ASSOCIATE, I.R.E.

Summary—*The ratio of the reactance to resistance of a coil or condenser may be expressed as its Q. Direct-reading instruments for this measurement are commercially available. The theory of their operation is given and includes corrections to increase the accuracy of the results of the measurements.*

I. Introduction

IN communication engineering, Q the ratio of effective reactance to resistance at any frequency has great significance as a figure of merit of a coil or a condenser.

* Decimal classification: R202. Original manuscript received by the Institute March 6, 1942.

† Government of Madras Kilpauk Post Office, Madras, South India.

Q for a coil, denoted by Q_L, $= \dfrac{\omega L_{eff}}{R_{eff}}$

and Q for a condenser, denoted by Q_C, $= \dfrac{1}{\omega C_{eff} R_{eff}}$, where

L_{eff}, C_{eff}, R_{eff} are the effective values at the specified frequency f $(\omega=2\pi f)$.

In order to evaluate the Q of a coil at different high frequencies, one has to measure carefully both L_{eff} and R_{eff} at each frequency and calculate the corresponding values of Q. To obviate this laborious process, a few British and American firms have recently marketed

a very ingenious and versatile meter called the circuit-magnification or Q meter, on which values of Q between 10 and 500 can be read directly for frequencies between 50 kilocycles and 50 or even 75 megacycles. The accuracy of measurement of the Q value in the Marconi-Ekco Q meter, Type TF 329D, is ± 5 per cent ± 5 up to 10 megacycles. Its frequency range is from 50 kilocycles to 50 megacycles. The versatility of the meter will be seen from the following list of measurements that can be made with such a meter;

1) Q of coils and condensers
2) Self-capacitance of coils
3) Inductance of coils
4) Capacitance of condensers
5) Power factor of condensers
6) Dielectrics and high resistances
7) Low impedances
8) Transmission-line constants
   a) Characteristic impedance
   b) Attenuation constant
   c) Wave velocity

II. Theory

A simple theory of this meter is worked out below. Fig. 1 shows the simplified circuit of a Q meter and Fig. 2, its equivalent circuit. S is an oscillator covering

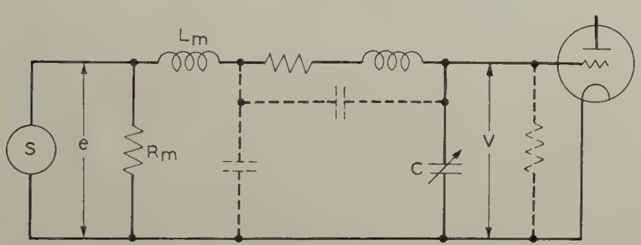

Fig. 1—Simplified circuit of a Q meter.

the desired frequency range and injecting a constant voltage e into the tuned circuit by means of the resistance R_m (0.04 ohm in the Marconi-Ekco meter). V is a valve voltmeter, measuring the voltage across the condenser for convenience. Actually, at resonance, the voltage across the coil and that across the condenser are equal in magnitude. R_a and L_a represent

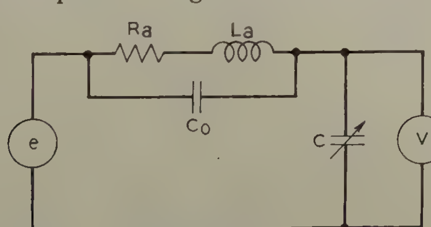

Fig. 2—Equivalent circuit of a Q meter.

the apparent values of resistance and inductance, and C_0, the self-capacitance of the coil, at the frequency in question. R_a and L_a are lumped so as to include R_m, the internal resistance, and L_m, the internal inductance of the source—the meter.

The apparent Q of the coil is given approximately by the ratio V/e, when the coil is tuned to resonance by the variable condenser C. When e is a known and fixed value (say, 20 millivolts), the valve voltmeter V, can be calibrated to read Q directly as shown below.

Let i be the current in the series circuit. Then

$$i = \frac{e}{R_a + j\omega L_a + \dfrac{1}{j\omega C}}.$$

If

$$Z_a = R_a + j\omega L_a, \quad i = \frac{e}{Z_a + \dfrac{1}{j\omega C_0}} \text{ or } \frac{je\omega C_0}{1 + jZ_a\omega C_0} \tag{1}$$

and

$$V = i \times \frac{1}{j\omega C_0}. \tag{2}$$

On substituting in (2) the value of i obtained in (1) we get

$$V = \frac{e}{1 + jZ_a\omega C_0}. \tag{3}$$

But, by definition, magnification $= V/e$

Therefore,

$$\frac{V}{e} = \frac{1}{1 + jZ_a\omega C_0} = \frac{1}{1 + j\omega C_0(R_a + j\omega L_a)}$$
$$= \frac{1}{(1 - \omega^2 L_a C_0) + j\omega R_a C_0}. \tag{4}$$

At resonance, V is a maximum and, e being constant, V/e too is a maximum then.

But

$$\left(\frac{V}{e}\right)^2 = \frac{1}{(1 - \omega^2 L_a C_0)^2 + (\omega R_a C_0)^2}. \tag{5}$$

Let

$$D \equiv (1 - \omega^2 L_a C_0)^2 + (\omega R_a C_0)^2. \tag{6}$$

Then $(V/e)^2$ is a maximum when (V/e) is a maximum, and when $(V/e)^2$ is a maximum D should be a minimum. The condition for D to be a minimum is, $d(D)/dC_0 = 0$. On differentiating (6), and equating to zero, we get

$$2(1 - \omega^2 L_a C_0)(-\omega^2 L_a) + 2\omega^2 C_0 R_a^2 = 0. \tag{7}$$

This expression, on simplification gives

$$C_0 = \frac{L_a}{Z_a^2}. \tag{8}$$

Substituting this value of C_0 in (5) and simplifying the results,

$$\left(\frac{V}{e}\right)^2 = \left(\frac{Z_a}{R_a}\right)^2 \text{ or } \frac{V}{e} = \frac{Z_a}{R_a}, \text{ i.e., } \frac{V}{e} = \frac{R_a + j\omega L_a}{R_a}, \tag{9}$$

i.e.,

$$\frac{V}{e} = 1 + j\frac{\omega L_a}{R_a}. \tag{10}$$

Thus the valve-voltmeter deflection is proportional to $\sqrt{1+Q^2}=Q$. Hence the meter dial can be calibrated to give $\omega L_a/R_a$, which is the apparent Q of the coil.

III. Corrections

As stated already, the indication of the meter is not the true Q, but the apparent Q.

Foster and Newlon[1] state that, for the meter they used, corrections for the following conditions were required for measurements above 9 megacycles:

1) Loading by the valve voltmeter
2) Internal impedance of the meter
3) Self-capacitance of the coil.

These corrections will be discussed.

1. Loading does not arise at all in the Marconi-Ekco meter, since the makers state that a special triode valve ($Ac/HL/DD$) having a very high input resistance was used.

2. The internal impedance of the meter consists of two factors, R_m the internal resistance, and L_m the internal inductance of the meter.

Q_t, the true Q of the coil, is given by

$$\frac{\omega L_t}{R_t} \tag{11}$$

and Q_a, the apparent Q of the coil, by

$$\frac{\omega L_a}{R_a}. \tag{12}$$

But,

$$L = L_a - L_m, \tag{13}$$

and

$$R_t = R_a - R_m. \tag{14}$$

Therefore,

$$\frac{Q_t}{Q_a} = \frac{\omega L_t}{R_t} \times \frac{R_a}{\omega L_a} = \frac{L_t}{L_a} \times \frac{R_a}{R_t}$$

or

$$Q_t = Q_a \frac{(L_a - L_m)}{L_a} \times \frac{R_a}{(R_a - R_m)}. \tag{15}$$

Evaluation of L_a and L_t is reached as follows: L_a is obtained from the meter readings. Since

$$f = \frac{1}{2\pi\sqrt{L_a(C+C_0)}}, \tag{16}$$

at resonance,

$$L_a = \frac{1}{4\pi^2 f^2(C+C_0)}, \tag{17}$$

where f is the frequency of the oscillator as read on the frequency calibration scale, C is the condenser reading on the meter, and C_0, the self-capacitance, which can be evaluated either by the negative-intercept method (from the graph of $(1/f^2)$ versus C or otherwise.

If f is in megacycles and C and C_0 are in micro-microfarads, L_a in microhenrys is obtained by

$$\frac{25{,}330}{f^2(C+C_0)} \tag{18}$$

and the true inductance

$$L \text{ (in microhenries)} = \frac{25{,}330}{f^2(C+C_0)} - L_m. \tag{19}$$

$L_m = 0.05$ microhenry in the Marconi-Ekco meter which the author used, and may even be neglected when L_a is comparatively large as that Q meter can measure the inductance of coils in the range 5 microhenries to 25 millihenries, approximately, with an accuracy of ± 3 per cent.

Thus, if L_m is neglected, then (15) reduces to

$$Q_t = Q_a \frac{R_a}{R_a - R_m}. \tag{20}$$

The need for the correction factor $R_a/(R_a - R_m)$ will depend solely on the relative values of R_a and R_m. If $R_m = 0.04$ ohm and R_a is of the order of even a few ohms, then $R_a/(R_a - R_m) \doteqdot 1$, and this correction also can be ignored without appreciable error.

3. The correction for the self-capacitance of the coil is by far the most important correction, which should be applied below 15 megacycles.

An expression for this correction is derived as follows. If f_0 is the natural frequency of the coil and f is the frequency at which Q is measured, then

$$f_0 \doteqdot \frac{1}{2\pi\sqrt{LC_0}} \quad \text{and} \quad f \doteqdot \frac{1}{2\pi\sqrt{LC}}. \tag{21}$$

Let k^2 denote the ratio

$$\frac{\omega^2}{\omega_0^2} = \left(\frac{f}{f_0}\right)^2 = \frac{C_0}{C}.$$

Further,

$$\frac{1}{\omega_0^2} \doteqdot LC_0, \tag{22}$$

Therefore,

$$\frac{\omega^2}{\omega_0^2} \doteqdot \omega^2 LC_0 \doteqdot k^2$$

It is well known that the effective inductance L_a and resistance R_a of a coil at a frequency $\omega = 2\pi f$, are approximately given by the following expressions,[2] where L and R are the physical or absolute values of inductance and resistance of the coil, respectively. These apparent values at a frequency f are a consequence of

[1] Dudley E. Foster and Arthur E. Newlon, "Measurement of iron cores at radio frequencies," Proc. I.R.E., vol. 29, pp. 269, 274–275; May, 1941.

[2] "Radio Instruments and Measurements" Bureau of Standards Circular C74, 1937, p. 133.

the self-capacitance C_0 of the coil. Fig. 3 shows the equivalent circuit at high frequencies of a coil having

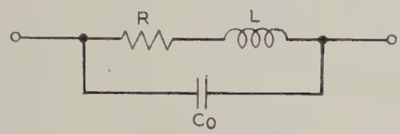

Fig. 3—Equivalent circuit of a coil at high frequencies.

resistance and distributed or self-capacitance.

$$L_a = \frac{L}{1 - \omega^2 L C_0} \tag{23}$$

and

$$R_a = \frac{R}{(1 - \omega^2 L C_0)^2}. \tag{24}$$

Substituting these values of L_a and R_a in (12) we get

$$Q_a = \frac{\omega L (1 - k^2)^2}{R(1 - k^2)} = \left(\frac{\omega L}{R}\right)(1 - k^2),$$

i.e.,

$$Q_a = Q(1 - k^2) \qquad \left(\text{since } Q = \frac{\omega L}{R}\right).$$

Therefore,

$$\text{actual } Q = \frac{Q_a}{1 - k^2}. \tag{25}$$

But $k^2 = C_0/C$ as is proved in (22).
Therefore,

$$Q = \frac{Q_a}{1 - \dfrac{C_0}{C}} = Q_a\left(\frac{C}{C - C_0}\right) \text{ or } Q_a\left(1 - \frac{C_0}{C}\right)^{-1}. \tag{26}$$

Expanding $(1 - C_0/C)^{-1}$ and neglecting the terms beyond the second we get

$$Q = Q_a\left(1 + \frac{C_0}{C}\right), \tag{27}$$

which is the only important correction below 15 megacycles.

IV. Order of Applying Corrections

After having ruled out the necessity for correction as a result of the valve-voltmeter loading, if more than one correction is required, they should be made in the following order.

1) Internal impedance of the meter
2) Self-capacitance of the coil.

At each stage the partially corrected values of Q and L should be used for the apparent value of $Q(Q_a)$ and $L(L_a)$ in the succeeding correction.

Some Aspects of Coupled and Resonant Circuits*

JESSE B. SHERMAN†, ASSOCIATE, I.R.E.

Summary—*An analysis is presented of the coupled impedance and its components in the two-mesh, inductively coupled circuit with a tuned secondary. A similar analysis is made of the impedance and its components in the parallel-resonant circuit having dissipation in the inductive branch.*

I. Introduction

It is well known that in the neighborhood of resonance the effect of the secondary circuit of Fig. 1 is similar to that of a parallel-resonant circuit in series with the primary. It is the purpose of this paper to examine the nature both of the coupled impedance in such a circuit and of the parallel-circuit impedance (Fig. 2). By expressing all of the quantities involved as general functions of a frequency ratio, the results can be presented graphically with relatively little labor of computation.

It is assumed that the circuits have constant resistance rather than constant Q.

II. Coupled Impedance

The mesh equations for the circuit of Fig. 1 (a) are

$$I_1 Z_1 + j\omega M I_2 = E_1 \tag{1}$$

$$I_2 Z_2 + j\omega M I_1 = 0. \tag{2}$$

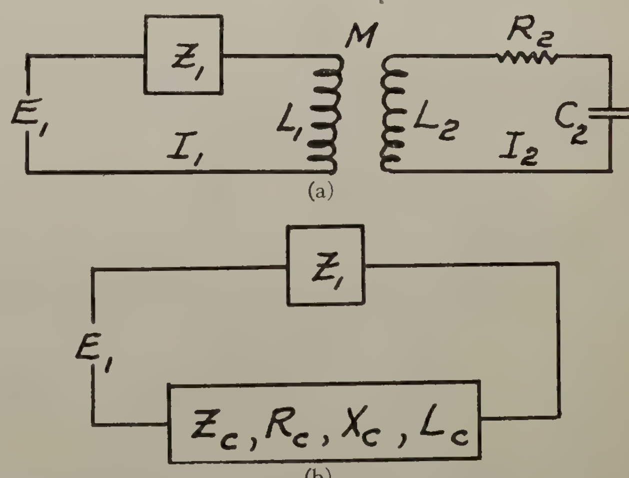

Fig. 1—Inductively coupled circuit with tuned secondary.

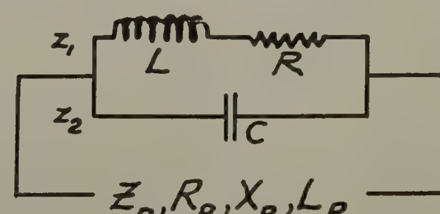

Fig. 2—Parallel circuit.

* Decimal classification: R142. Original manuscript received by the Institute, April 13, 1942.
† Electrical Engineering Department, The Cooper Union, New York, N. Y.

Solution for I_1 yields

$$I_1 = \frac{E_1}{Z_1 + (\omega M)^2/Z_2}. \tag{3}$$

The second term of the denominator represents the coupled impedance. This is

$$Z_c = \frac{\omega^2 M^2}{R_2 + j(\omega L_2 - 1/\omega C_2)} \tag{4}$$

or

$$|Z_c|^2 = \frac{\omega^6 C_2^2 M^4}{\omega^2 C_2^2 R_2^2 + (\omega^2 L_2 C_2 - 1)^2}. \tag{5}$$

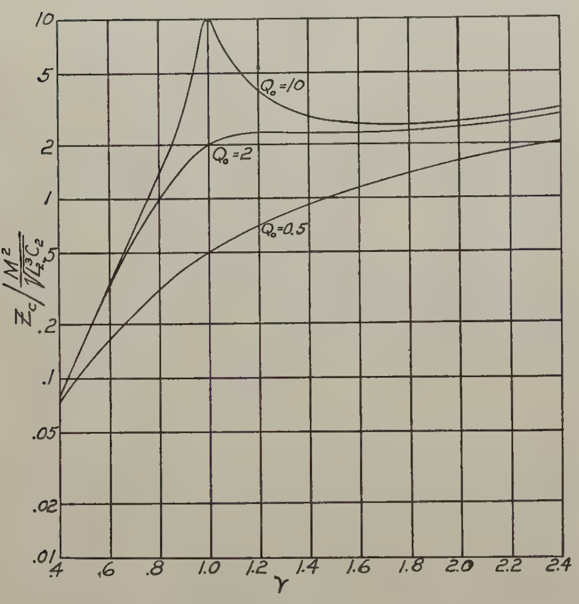

Fig. 3—Coupled impedance.

Making the substitution $\gamma = \omega/\omega_0$, and noting that $\omega_0^2 L_2 C_2$ and its powers are equal to unity, (5) can be written

$$|Z_c|^2 = \frac{M^4}{L_2^3 C_2} \cdot \frac{\gamma^6}{\gamma^4 + \alpha\gamma^2 + 1} \tag{6}$$

where $\alpha = 1/Q_0^2 - 2$. Maximizing (6) with respect to γ yields

$$\gamma^4 + 2\alpha\gamma^2 + 3 = 0 \tag{7}$$

whence

$$\gamma = \pm\sqrt{2 - \frac{1}{Q_0^2} \pm \sqrt{1 - \frac{4}{Q_0^2} + \frac{1}{Q_0^4}}}. \tag{8}$$

Inspection of (8) indicates that when Q_0 is large there will be two real positive values of γ:

$$\gamma_1 = 1 \tag{9a}$$

and

$$\gamma_2 = \sqrt{3}. \tag{9b}$$

Whether these are maxima or minima remains to be seen. It also appears that there will be a single positive value of γ when

$$1 - \frac{4}{Q_0^2} + \frac{1}{Q_0^4} = 0. \tag{10}$$

Solution for this boundary value of Q yields as the only usable root

$$Q_0 = \sqrt{2 + \sqrt{3}} \tag{11}$$

and substitution of (11) in (8) gives

$$\gamma_3 = \sqrt[4]{3} \tag{12}$$

If we now plot $Z_c\sqrt{L_2^3 C_2/M^2}$ from (6) as a function of γ for several values of Q_0 we obtain the curves of Fig. 3. Examination of Fig. 3 and the above relations shows that the coupled impedance for large Q_0 has a

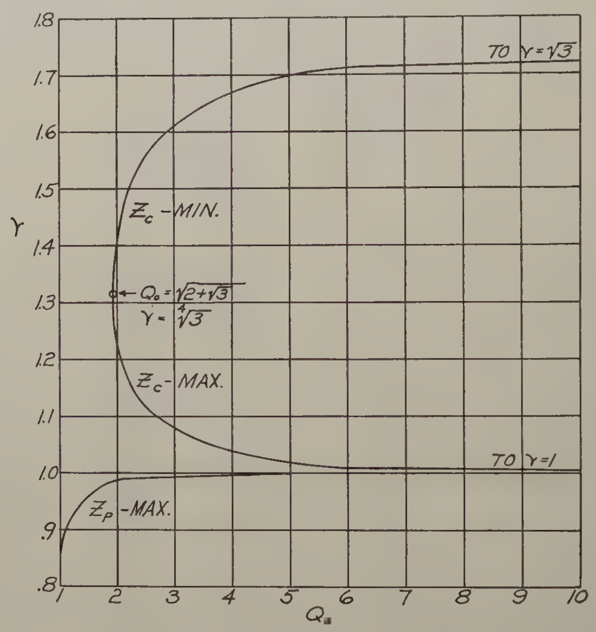

Fig. 4—Loci of impedance maxima.

maximum at $\gamma_1 = 1$ and a minimum at $\gamma_2 = \sqrt{3}$. As Q_0 is reduced these points converge to an inflection at γ_3, the geometric mean of γ_1 and γ_2, for which $Q_0 = \sqrt{2+\sqrt{3}}$. For smaller values of Q_0 the function rises continuously. The loci of the maximum and minimum are plotted from (8), in Fig. 4.

III. Coupled Resistance

Expansion of (4) yields

$$Z_c = \frac{(\omega M)^2}{Z_2^2} R_2 - j\frac{(\omega M)^2}{Z_2^2} X_2. \tag{13}$$

The resistance component of (13) is

$$R_c = \frac{\omega^2 M^2 R_2}{R_2^2 + (\omega L_2 - 1/\omega C_2)^2} \tag{14}$$

which can be written as

$$R_c = \frac{M^2 R_2}{L_2^2} \cdot \frac{\gamma^4}{\gamma^4 + \alpha\gamma^2 + 1}. \tag{15}$$

Maximizing (15) with respect to γ gives

$$\gamma^2 + 2/\alpha = 0 \tag{16}$$

whence

$$\gamma = \frac{1}{\sqrt{1 - 1/2Q_0^2}} \cdot \tag{17}$$

That is, the coupled resistance displays a maximum if $Q_0 > 1/\sqrt{2}$.

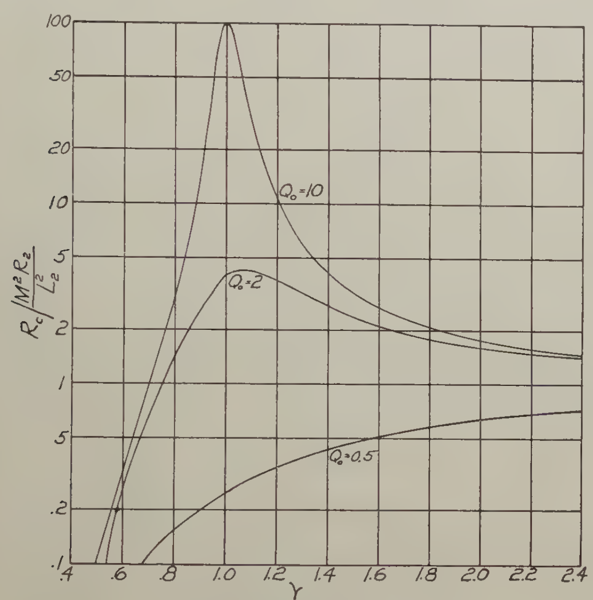

Fig. 5—Coupled resistance.

$R_c \times L_2/M^2R_2$ from (15) is plotted for several values of Q_0 in Fig. 5. The locus of the maximum is plotted as a function of Q_0 from (17), as the upper curve of Fig. 6.

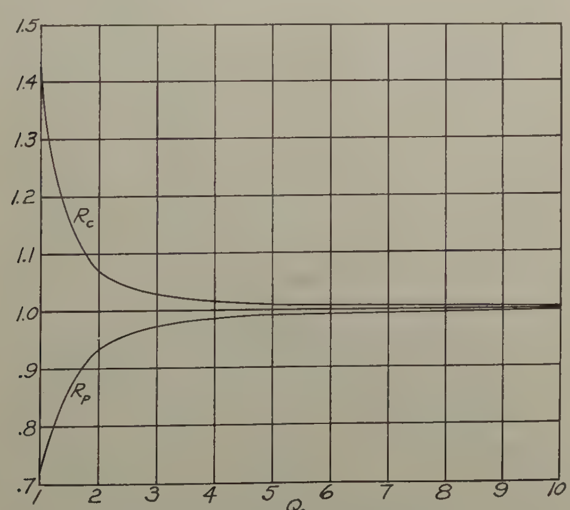

Fig. 6—Loci of resistance maxima.

IV. Coupled Reactance

The reactance component of (13) is

$$X_c = \frac{\omega^3 M^2 C_2 - \omega^5 M^2 C_2^2 L_2}{\omega^2 C_2^2 R_2^2 + (\omega^2 L_2 C_2 - 1)^2} \tag{18}$$

which can be recast as

$$X_c = \frac{\omega_0 M^2}{L_2} \cdot \frac{\gamma^3 - \gamma^5}{\gamma^4 + \alpha\gamma^2 + 1} \cdot \tag{19}$$

The coupled reactance is plotted in Fig. 7 for several values of Q_0. As evident from (19), the coupled reactance is always zero at $\gamma = 1$, regardless of Q_0.

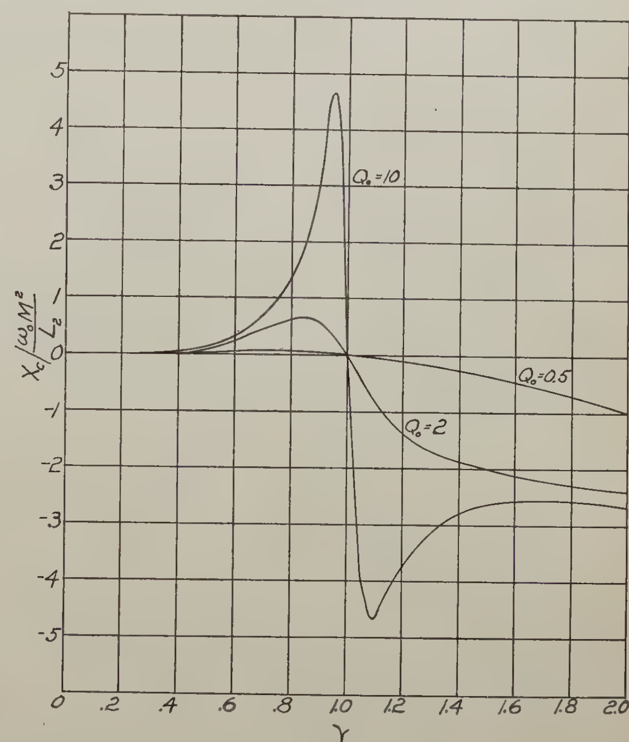

Fig. 7—Coupled reactance.

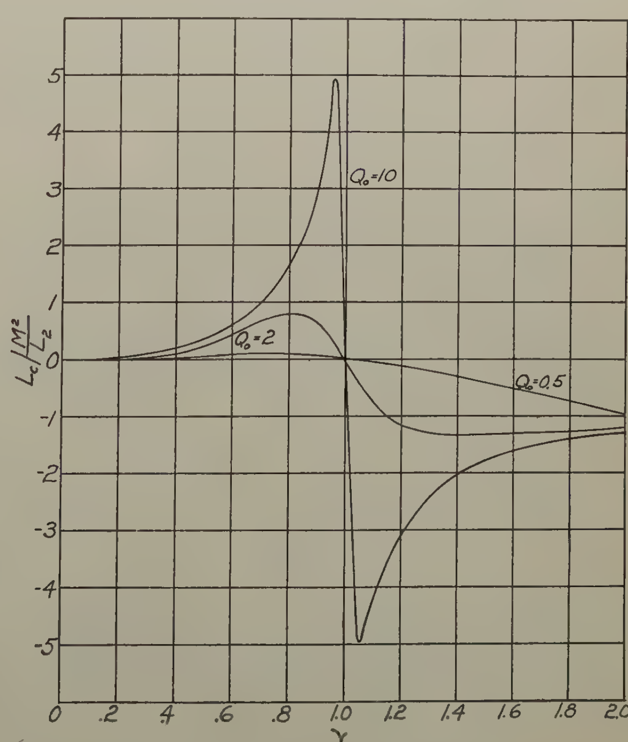

Fig. 8—Effective coupled inductance.

V. Effective Coupled Inductance

Equation (19) represents an effective inductance X_c/ω. Hence the effective coupled inductance is

$$L_c = \frac{M^2}{L_2} \cdot \frac{\gamma^2 - \gamma^4}{\gamma^4 + \alpha\gamma^2 + 1}. \tag{20}$$

Maximizing with respect to γ gives

$$(\alpha + 1)\gamma^4 + 2\gamma^2 - 1 = 0 \tag{21}$$

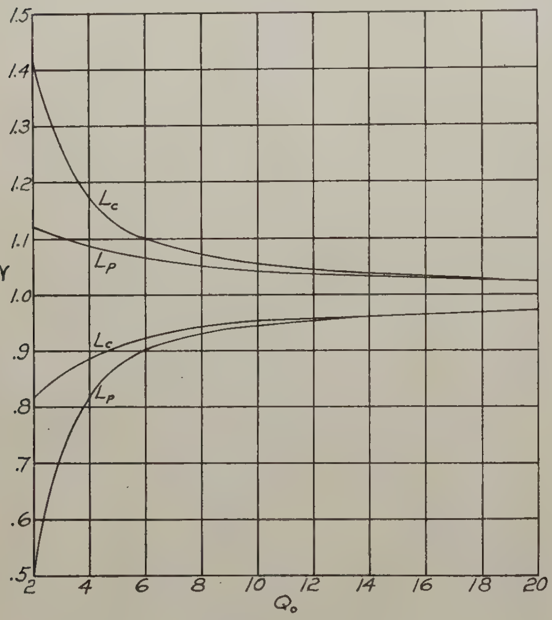

Fig. 9—Loci of effective inductance maxima.

whence

$$\gamma_1 = \sqrt{\frac{Q_0}{Q_0 + 1}} \tag{22a}$$

and

$$\gamma_2 = \sqrt{\frac{Q_0}{Q_0 - 1}}. \tag{22b}$$

These expressions are the loci of the maximum and minimum respectively of (20), and indicate that a maximum will always occur, and a minimum will occur if $Q_0 > 1$. Equation (20) is plotted in Fig. 8, and the loci are plotted as the L_c curves of Fig. 9. As with the coupled reactance, the effective coupled inductance is always zero at $\gamma = 1$, regardless of Q_0.

VI. Parallel Impedance

The impedance of the circuit of Fig. 2 is

$$Z_p = \frac{z_1 z_2}{z_1 + z_2}. \tag{23}$$

On making the indicated branch substitutions, expanding, and squaring, (23) becomes

$$|Z_p|^2 = \frac{R^2 + \omega^2 L^2}{\omega^2 C^2 R^2 + (\omega^2 LC - 1)^2}. \tag{24}$$

This can be written

$$|Z_p|^2 = R^2 \frac{1 + Q_0^2\gamma^2}{\gamma^4 + \alpha\gamma^2 + 1}. \tag{25}$$

Maximizing with respect to γ and solving yields

$$\gamma = \sqrt{\sqrt{1 + 2/Q_0^2} - 1/Q_0^2}. \tag{26}$$

The boundary condition for (26) is

$$\sqrt{1 + 2/Q_0^2} = 1/Q_0^2 \tag{27}$$

whence

$$Q_0 = \sqrt{\sqrt{2} - 1}. \tag{28}$$

That is, Z_p^2 (and hence Z_p) will display a maximum if $Q_0 > \sqrt{\sqrt{2} - 1}$. Z_p/R is plotted from (25) in Fig. 10 for several values of Q_0. When Q_0 is less than the value given by (28), the impedance characteristic degenerates to that of a capacitance and resistance in parallel. Fig. 10 should be compared with Fig. 3. When Q_0 is large the coupled impedance and parallel impedance show similarity in the vicinity of $\gamma = 1$.

The locus of the maximum parallel impedance is plotted from (26) as a function of Q_0, in Fig. 4.

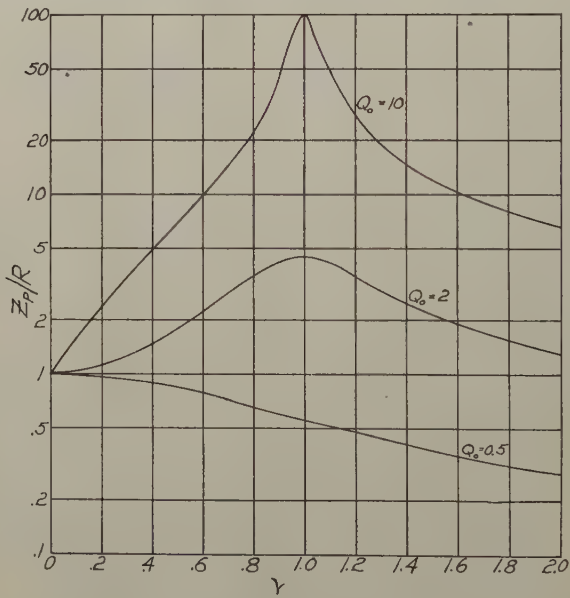

Fig. 10—Parallel-circuit impedance.

VII. Parallel-Circuit Resistance

The impedance expression (23) yields on expansion

$$Z_p = \frac{R/\omega^2 C^2}{R^2 + (\omega L - 1/\omega C)^2} + j\frac{L/\omega C^2 - \omega L^2/C - R^2/\omega C}{R^2 + (\omega L - 1/\omega C)^2}. \tag{29}$$

The resistance component of (29) can be written as

$$R_p = R \frac{1}{\gamma^4 + \alpha\gamma^2 + 1}. \tag{30}$$

Maximizing with respect to γ gives

$$\gamma^2 + \alpha/2 = 0 \tag{31}$$

whence

$$\gamma = \sqrt{1 - 1/2Q_0^2} \tag{32}$$

which is the reciprocal of the expression for the locus of the maximum coupled resistance, and also displays a maximum for $Q_0 > 1/\sqrt{2}$. R_p/R from (30) is plotted in Fig. 11, and the locus is plotted from (32) as the lower curve of Fig. 6.

VIII. Parallel-Circuit Reactance

The reactance component of (29) is

$$X_p = \frac{\omega L - \omega^3 L^2 C - R^2 \omega C}{\omega^2 C^2 R^2 + (\omega^2 LC - 1)^2}. \tag{33}$$

This can be recast as

$$X_p = \omega_0 L \frac{\delta\gamma - \gamma^3}{\gamma^4 + \alpha\gamma^2 + 1} \tag{34}$$

where $\delta = 1 - 1/Q_0^2$. Equation (34) is plotted in Fig. 12. The reactance has a fixed value of $-\omega_0 L$ at $\gamma = 1$, regardless of Q_0 (provided Q_0 is finite); and is equal to

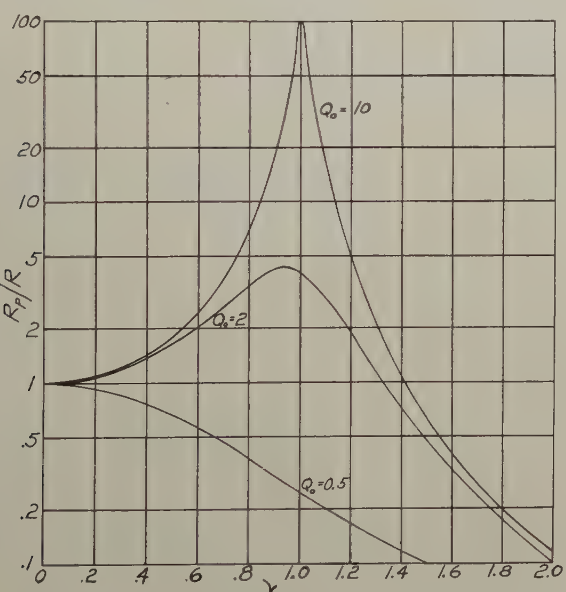

Fig. 11—Parallel-circuit resistance.

zero at some point below $\gamma = 1$, dependent on Q_0. This resonant point (i.e., unity power factor), is found by setting the numerator of (34) equal to zero:

$$\delta\gamma - \gamma^3 = 0 \tag{35}$$

whence

$$\gamma = \sqrt{1 - 1/Q_0^2}. \tag{36}$$

(It can be shown that when the resistance occurs only in the capacitive branch of the parallel circuit, the reactance has a fixed value of $+\omega_0 L$ at $\gamma = 1$; and when equal resistance is present in both branches, the reactance is zero at $\gamma = 1$.)

IX. Effective Inductance of the Parallel Circuit

Equation (34) represents an effective inductance X_p/ω. Thus the effective inductance is

$$L_p = L \frac{\delta - \gamma^2}{\gamma^4 + \alpha\gamma^2 + 1}. \tag{37}$$

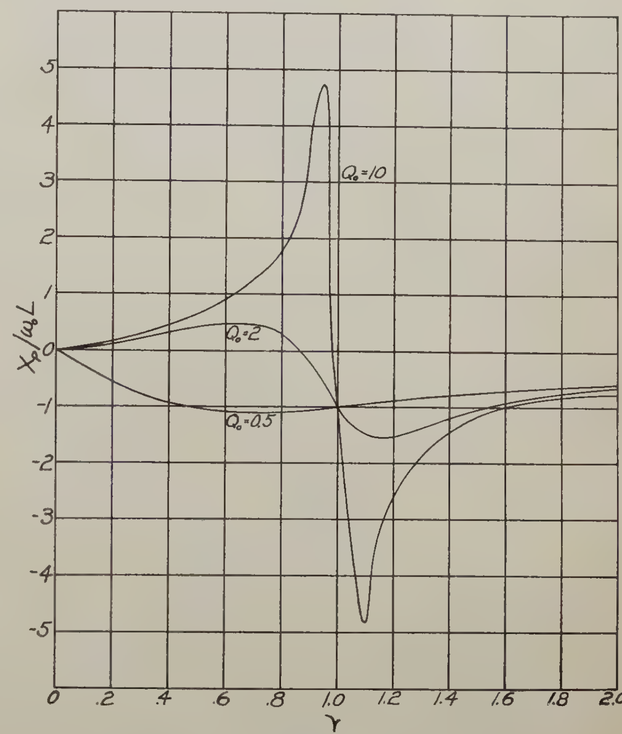

Fig. 12—Parallel-circuit reactance.

Maximizing (37) with respect to γ gives

$$\gamma_1 = \sqrt{1 - 1/Q_0^2 - 1/Q_0} \tag{38a}$$

and

$$\gamma_2 = \sqrt{1 - 1/Q_0^2 + 1/Q_0}. \tag{38b}$$

The first is the maximum, which occurs for $Q_0 > 1.62$. The second is the minimum, which occurs for $Q_0 > 0.62$. The loci of maximum and minimum are plotted in Fig. 9. Equation (37) is plotted in Fig. 13. The effective inductance is zero (for sufficient Q_0) at a frequency found by setting the numerator of (37) equal to zero:

$$\delta - \gamma^2 = 0 \tag{39}$$

whence

$$\gamma = \sqrt{1 - 1/Q_0^2} \tag{40}$$

which has already been found to be the point of unity power factor.

It should be observed that (37) and Fig. 13 do not hold for zero frequency, at which the effective inductance in this circuit cannot differ from L.

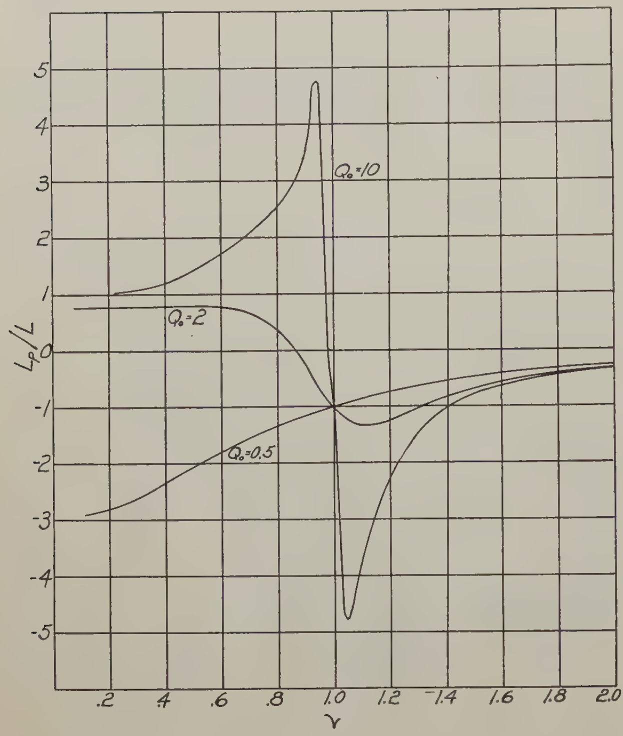

Fig. 13—Effective inductance of parallel circuit.

X. Series-Circuit Note

It is of interest to note that equations (17) and (32) also give respectively the locus of the maximum inductance and capacitance voltage in a series-resonant

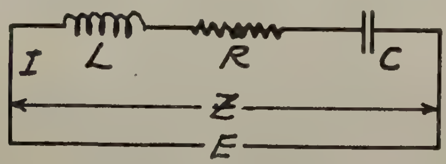

Fig. 14—Series circuit.

circuit. Thus, referring to Fig. 14, the voltage across the inductance is

$$E_L=\omega LI=\frac{E}{Z}\omega L=E\frac{\omega L}{\left[R^2+\left(\frac{\omega^2LC-1}{\omega C}\right)^2\right]^{1/2}} \tag{41}$$

which can be cast into the form

$$E_L = E\frac{\gamma^2}{(\gamma^4+\alpha\gamma^2+1)^{1/2}}\cdot \tag{42}$$

This frequency function is the square root of that of (15). Hence, maximizing (42) with respect to γ also yields (17).

Similarly, the voltage across the capacitance is

$$E_c=\frac{I}{\omega C}=\frac{E}{\omega CZ}=\frac{1/\omega C}{\left[R^2+\left(\frac{\omega^2LC-1}{\omega C}\right)^2\right]^{1/2}} \tag{43}$$

which can be recast as

$$E_c = E\frac{1}{(\gamma^4+\alpha\gamma^2+1)^{1/2}}\cdot \tag{44}$$

This frequency function is the square root of that of (30). Hence, maximizing (44) with respect to γ also gives (32).

Acknowledgment

The author is indebted to Mr. Hugo J. Di Giovanni of this staff for his assistance in obtaining experimental data in connection with this paper.

Appendix

Nomenclature

I_1 = primary current
I_2 = secondary current
Z_1 = impedance of the isolated primary
Z_2 = impedance of the isolated secondary.
M = mutual inductance
E_1 = applied primary voltage
L_2 = secondary inductance
C_2 = secondary capacitance
R_2 = secondary resistance (assumed constant)
L = inductance of the parallel or series circuit
C = capacitance of the parallel or series circuit
R = resistance of the parallel or series circuit (assumed constant)
Z_c = coupled impedance
R_c = coupled resistance
X_c = coupled reactance
L_c = effective coupled inductance
Z_p = impedance of the parallel circuit
R_p = resistance component of parallel circuit impedance
X_p = reactance component of parallel circuit impedance
L_p = effective inductance of the parallel circuit
I = current in the series circuit
E = applied voltage in the series circuit
E_c = capacitance voltage in the series circuit
E_L = inductance voltage in the series circuit
$\omega = 2\pi\times$frequency
$\omega_0 = 2\pi\times$frequency at which $\omega L_2 = 1/\omega C_2$ or $\omega L = 1/\omega C$
$\gamma = \omega/\omega_0$
$Q_0 = \omega_0 L_2/R_2$ or $\omega_0 L/R$
$\alpha = 1/Q_0^2 - 2$
$\delta = 1 - 1/Q_0^2$

On Radiation from Antennas*

S. A. SCHELKUNOFF†, ASSOCIATE, I.R.E., AND C. B. FELDMAN†, ASSOCIATE, I.R.E.

Summary—This paper presents some theoretical remarks and experimental data relating to applications of the transmission-line theory to antennas. It is emphasized that the voltage, the current, and the charge are affected by radiation in different ways, a fact which should be considered in any adaptation of line equations to antennas.

It is shown experimentally and theoretically that in an antenna of length equal to an integral number of half wavelengths, which is energized at a current antinode, the effect of radiation on the current and the charge (but not on the voltage) can roughly be represented by adding to the resistance of the wires another fairly simple term.

I. General Discussion

FOR MANY years it has been known that the current distribution in an antenna approximates that obtained by regarding the antenna as an open-circuited transmission line with certain series inductance and shunt capacitance per unit length. In other words, it has been known that effects of radiation on the current distribution are relatively small. During the last decade much thought has been given to improving upon this approximate picture by an inclusion of radiation effects, while remaining within the framework of the transmission-line theory. A theoretical question is whether or not such an improvement is possible within the limits of the line theory. While experimentally minded engineers, not being particularly worried by such questions, have achieved a measure of success, theoreticians have been beset with doubts. These doubts are only natural, since the only safe mathematical approach to the problem is through Maxwell's field equations, and these apparently make the antenna problem quite different from line problems.

In the line theory we write

$$\frac{dV}{dx} = -(R + i\omega L)I, \quad \frac{dI}{dx} = -(G + i\omega C)V, \tag{1}$$

where V and I are the voltage across the line and the current in it; the line parameters R, L, G, and C are, respectively, the series resistance, the series inductance, the shunt conductance, and the shunt capacitance, all per unit length. In applying these equations to a pair of parallel wires (Fig. 1), we say that R is the

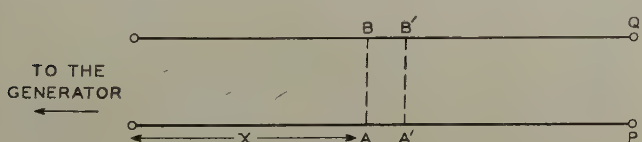

Fig. 1

resistance of the wires per unit length and that it represents the power dissipated in heat. If the medium surrounding the wires is nondissipative, we say that G is equal to 0. We define C as the ratio of the electric charge per unit length to the voltage across the line. The quantity "$i\omega LI$" is the counterelectromotive force of induction in "series" with the wires; it represents the reaction of the changing magnetic flux between the wires on the line voltage. This is the picture if radiation is ignored; and if we ignore radiation, there is nothing to prevent us from applying the picture to diverging wires (Figs. 2 and 3). If there is any difference between the three structures in Figures 1, 2, and 3, it is in the magnitude of radiation effects.

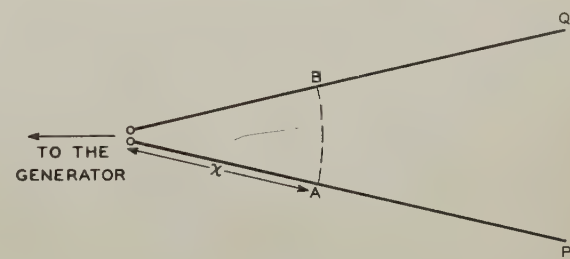

Fig. 2

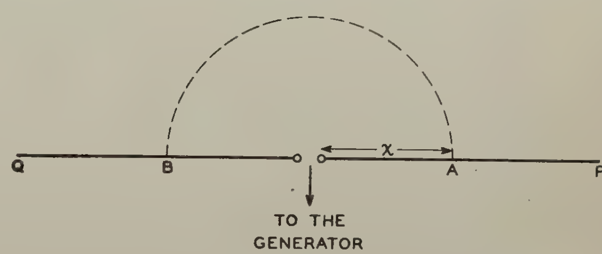

Fig. 3

One of the effects of dissipation is to cause attenuation of the voltage and current waves. Since radiation represents additional loss of power, it has been thought that it should cause further attenuation. In order not to confuse the issue, let us assume, for the time being, that the wires are perfectly conducting and that the surrounding medium is nondissipative; then, if R and G are different from 0, they must represent the effect of radiation.

One line of thought runs somewhat as follows. Ignoring radiation and solving (1) we find the first approximation to the current distribution $I(x)$ and charge distribution $q(x)$. Using this current distribution, we compute the retarded electric potential U and the retarded magnetic vector potential Π

$$U(x) = \frac{1}{4\pi\epsilon}\int \frac{q(x')e^{-i\beta r}}{r}\,dx', \qquad \Pi(x) = \frac{1}{4\pi}\int \frac{I(x')e^{-i\beta r}}{r}\,dx', \tag{2}$$

where the integration is extended over the wires;

* Decimal classification: R120. Original manuscript received by the Institute, December 31, 1941.

† Bell Telephone Laboratories, Inc., New York, N. Y.

$\beta = 2\pi/\lambda = \omega/c$; and r is the distance between the current element $I(x')dx'$ and a typical point in space

$$r = \sqrt{(x' - x)^2 + \rho^2}, \qquad \rho^2 = y^2 + z^2. \qquad (3)$$

Strictly speaking, the integrals should be taken over the surface of the wires; but if the wires are thin, good approximations are given by (2).

From U and Π we compute the field with the aid of the following equations

$$E = i\omega\mu\Pi - \text{grad } U, \qquad H = \text{curl } \Pi. \qquad (4)$$

Next, we obtain the total radiated power by forming the Poynting vector $E \times H$ and integrating it over a surface enclosing the antenna.

At this point we usually leave the solid ground and make the following *à priori* physical assumptions: (1) Equations (1) *can* take care of radiation, (2) the effect of radiation is expressed solely by a series resistance R_{rad}, and (3) R_{rad} is uniform. Granting tentatively these assumptions, we can compute R_{rad} so that the integral of $R_{\text{rad}} I^2$ along the antenna is equal to the radiated power. We can now use (1) for recomputing the current distribution. P. O. Pedersen[1] used this procedure and obtained a current distribution which checked rather well the measured current distribution.

Nevertheless, not all is well with this procedure. Let us examine the three *à priori* assumptions. There are no logical objections to the first assumption, if we permit R, L, G, and C to vary in any manner with x; since V and I are definite functions of x, we can always use (1) as *definitions* of the line parameters. Naturally, these equations are useless for computing V and I unless we can find R, L, G, and C by independent means; but utility, or lack of it, does not affect the assumption. However, the second assumption, G_{rad} equals 0, is incorrect. It can be shown that V is not affected by radiation and that the ratio of dI/dx to V is a complex number.

This difficulty can be obviated if we write our transmission equations in terms of electric charge $q(x)$ and electric current $I(x)$ rather than the voltage-current form (1). In the first place, we have the equation of conservation of electric charge

$$\frac{dI}{dx} = -i\omega q, \qquad (5)$$

which takes place at the second equation in (1). Next, we define V arbitrarily so that $C = q/V$ is independent of x and, finally, we write the first equation of (1) as follows

$$\frac{dq}{dx} = -(R_{\text{rad}}C + i\omega LC)I. \qquad (6)$$

Of course, V as defined above is fictitious; but then it does not appear in our ultimate equations (5) and (6) and we need not be concerned with it. Besides, the measurements are carried out on q and I.

In an earlier paper by one of the present authors,[2] equation (6) was obtained directly from Maxwell's equations. There it was made clear that RC and LC were complicated functions of x.

Comparing the voltage-current transmission equations (1) to the current-charge equations (5) and (6), we observe that the latter are simpler in the sense that the "line" parameters enter into only one equation. Once we are certain that the form of equations (5) and (6) is permissible, we step on a more certain ground with regard to Pedersen's method of obtaining a second approximation to the current distribution in antennas. It appears that while radiation does not affect the voltage distribution in antennas, it affects the current and the charge in more or less the same manner that dissipation does.

Pedersen has assumed *ab initio* that R_{rad} is constant. In the third part of this paper we derive from Maxwell's equations the following approximate expression

$$R_{\text{rad}} = \frac{60l}{l^2 - x^2} \qquad (7)$$

for the case when the length $2l$ of the antenna (of the type shown in Fig. 3) is an integral number of half wavelengths and the generator is at a current antinode. This function is represented by the solid curve in Fig. 4, where the experimental points, obtained under various conditions, are also marked.

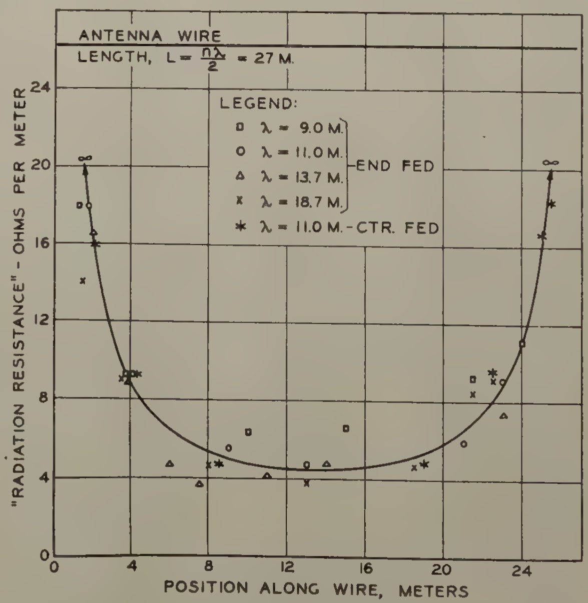

Fig. 4

For other antenna lengths, the formula becomes more complicated and indicates greatly increased radiation resistance near the current nodes.

[1] P. O. Pedersen, "Radiation from a vertical antenna over flat perfectly conducting earth," *Ingeniørvidenskabelige Skrifter*, ser. A, no. 38, 1935.

[2] S. A. Schelkunoff, "Theory of antennas of arbitrary size and shape," Proc. I.R.E., vol. 29, pp. 493–521; September, 1941.

Before proceeding with an account of our experiments and the mathematical derivation of (7), we shall, following another line of thought, give a descriptive resumé of a recent antenna theory[2] which is particularly useful for computing input impedances of antennas. Let us go back to (1) and write them in a form suitable to the nondissipative case

$$\frac{dV}{dx} = -i\omega LI, \qquad \frac{dI}{dx} = -i\omega CV. \tag{8}$$

These equations apply exactly to an infinitely long pair of conical conductors diverging from a common apex as shown in Figs. 2 and 3. In the limit, they apply to an infinitely long pair of parallel cylindrical wires. In any of the above cases L and C are constant. These equations will also apply with a high degree of accuracy to diverging cylindrical wires if the latter are thin; in this case, however, L and C will vary with the distance x.

The transverse voltage V is defined as the line integral of the electric intensity between the wires, taken along a path lying completely in an equiphase surface, that is, in a plane perpendicular to the parallel wires and in a sphere concentric with the apex of diverging wires.

Now let the wires terminate at P and Q. It turns out that if we subtract a certain "complementary" or "local" current $I_c(x)$ from the actual total current $I_t(x)$, the remainder $I(x)=I_t(x)-I_c(x)$ and the transverse voltage $V(x)$ will satisfy (8). The complementary current is 0 at the apex of the diverging wires; in the case of parallel wires, it diminishes as the distance from the terminals PQ increases. For the case of parallel wires this fact was noted by Carson.[3] Thus, the input impedance of diverging wires and long parallel pairs will be given as the ratio of the applied voltage to the "principal current" $I(0)$, the latter being equal to the total current $I_t(0)$.

The total current vanishes at P; hence, the principal current there becomes equal to $-I_c(P)$. The relation between the total voltage and the principal current at PQ is that which would be obtained if the complementary current were disregarded and in its stead a terminal impedance equal to $V(P)/-I_c(P)$ were assumed. This terminal impedance, which may be called the "radiation impedance," is a complex quantity, the real part of which represents the radiated power. For large values of the characteristic impedance, the radiation impedance is substantially proportional to the square of the characteristic impedance.

In the elementary theory, the complementary current and the complementary charge are ignored. In effect, this makes the terminal radiation impedance infinite and the transmission line becomes electrically "open." In the complete theory, the voltage remains sinusoidal, although the end of the line is no longer a voltage antinode; of the electric current and electric charge only the major parts are sinusoidal. The effect of the discontinuity of the line at PQ on these major parts is represented completely by the radiation impedance. The complete theory approaches the elementary theory as either the characteristic impedance or the wavelength becomes infinite.

In accordance with what has just been said, we are permitted to think that a wave emerging from a generator is guided by the wires until it reaches the ends where the transmission system suddenly changes;[4] there, reflection takes place. The amount of reflection is not the same at all points of the wavefront so that besides the reflected wave which is guided back to the generator, there appears a "complementary" field which compensates for the uneven reflection.

The uneven reflection may be pictured as follows. Consider the wavefront passing through the ends of the wires and apply Huygens' principle or, rather, its more explicit form known as the equivalence principle.[5-8] The secondary sources, near the wire but on its opposite sides, are 180 degrees out of phase. Being so near each other, their effect on the field beyond the antenna region is very small and they emit very little energy. But the energy arriving from the generator is denser near the wires than elsewhere; hence, the greatest reflection will occur over the area of the wavefront in the neighborhood of the wires.

The quantitative counterpart of the above qualitative antenna theory will be found in the paper[2] already referred to. The theory is sufficient for obtaining engineering information about performance of many different types of antennas.

We have just discussed several ways in which the line equations can be used in conjunction with the field equations in dealing with radiation problems. At present, the method which has been discussed last appears to be the most promising from the practical point of view and it possesses the theoretical advantage of being a child of the field theory. The earlier method is of interest largely because it shows that the old controversy as to whether radiation takes place continuously or "snaps off" the ends of the antenna is rather meaningless. One can look at it either way.

II. Experimental Part

The experiment concerns verification of (7). The method consists of exciting an elevated antenna wire with a transmitting oscillator, and measuring the shape of the nodes (minima) of current and charge. The total

[3] John R. Carson, "The guided and radiated energy in wire transmission," *Jour. A.I.E.E.*, pp. 906–913; October, 1924.

[4] The space with wires embedded in it is replaced by space without wires.

[5] S. A. Schelkunoff, "Some equivalence theorems of electromagnetics and their application to radiation problems," *Bell Sys. Tech. Jour.*, pp. 92–112; January, 1936.

[6] S. A. Schelkunoff, "On different fraction and radiation of electromagnetic waves," *Phys. Rev.*, pp. 308–316; August 15, 1939.

[7] S. A. Schelkunoff, "A general radiation formula," Proc. I.R.E., vol. 27, pp. 660–666; October, 1939.

[8] J. A. Stratton, "Electromagnetic Theory," McGraw-Hill Book Company, New York, N. Y. 1941, pp. 464–470.

attenuation suffered by a wave traveling to the open end and back to the node in question can be deduced from the nodal shape, assuming a constant characteristic impedance. Measurements made upon several nodes between the generator and the open end yield a curve of total attenuation versus position on the wire whose slope can be interpreted as the attenuation exponent for that position. In order to obtain the resistance from the attenuation exponent it is necessary to know the characteristic impedance. One method of measuring the characteristic impedance is to measure attenuation for two antennas whose ohmic resistances are different. Such a resistance variation permits the radiation effect to be subtracted out and the characteristic impedance to be calculated from the remaining attenuation. The theory underlying this method of measurement is as follows.

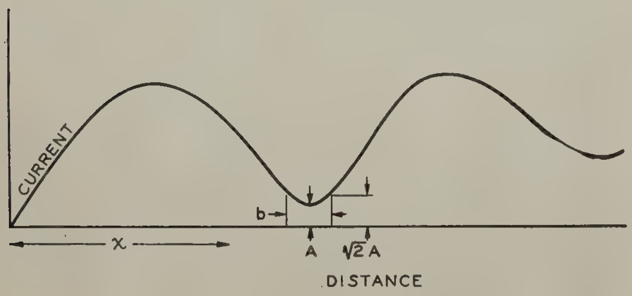

Fig. 5

Assuming that the resistance $R(x)$ of a transmission line is small compared with its characteristic impedance K, we can write an approximate expression for the current at distance x from one end of the wire (Fig. 5) in the form

$$I(x) = \sinh (A + i\beta x) \doteq A \cos \beta x + i \sin \beta x, \tag{9}$$

where $A(x)$ is the total attenuation to point x

$$A(x) = \frac{\int_0^x R(x)dx}{2K}. \tag{10}$$

From (10) we have

$$R(x) = 2K \frac{dA}{dx}. \tag{11}$$

The values of A corresponding to the current minima and charge minima can be related to the shape of the latter. Thus the minima of $I(x)$ are near points for which $\sin \beta x = 0$, so that minimum amplitudes are given by $A(x)$. The points for which the amplitudes are equal to $\sqrt{2}\ A$ occur where the real and the imaginary parts of (9) are equal; that is, (Fig. 5),

$$\sin \frac{\beta b}{2} = A \cos \frac{\beta b}{2}; \quad \text{or} \quad \frac{\beta b}{2} = A, \quad \text{or} \quad A = \frac{\pi b}{\lambda}. \tag{12}$$

Setting

$$\begin{aligned} A_1(x) &= \frac{\int_0^x R_{\text{rad}}(x)dx}{2K} \quad \text{for zero wire resistance} \\ A_2(x) &= \frac{\int_0^x R_{\text{rad}}(x)dx + rx}{2K} \quad \text{for resistance wire,} \end{aligned} \tag{13}$$

where r is the resistance per unit length, we obtain,

$$\begin{aligned} 2K &= \frac{rx}{A_2(x) - A_1(x)}, \\ R_{\text{rad}}(x) &= \frac{rx}{A_2(x) - A_1(x)} \frac{dA_1}{dx}. \end{aligned} \tag{14}$$

The test antenna was a No. 14 B & S gauge wire 27 meters long stretched horizontally under the roof of a large barn. Copper and Nichrome wires were used. A wooden platform erected 7 feet beneath the wire enabled an operator to carry apparatus with which to measure current and charge distribution. The current-measuring equipment employed a small loop highly balanced against response to potential gradient, while charge-measuring equipment employed a receiver with weak capacitive coupling to the antenna. Measurements were made at several wavelengths from 9 to 18 meters and with the oscillator coupled to the wire in various ways near one end and at the middle. A plot of

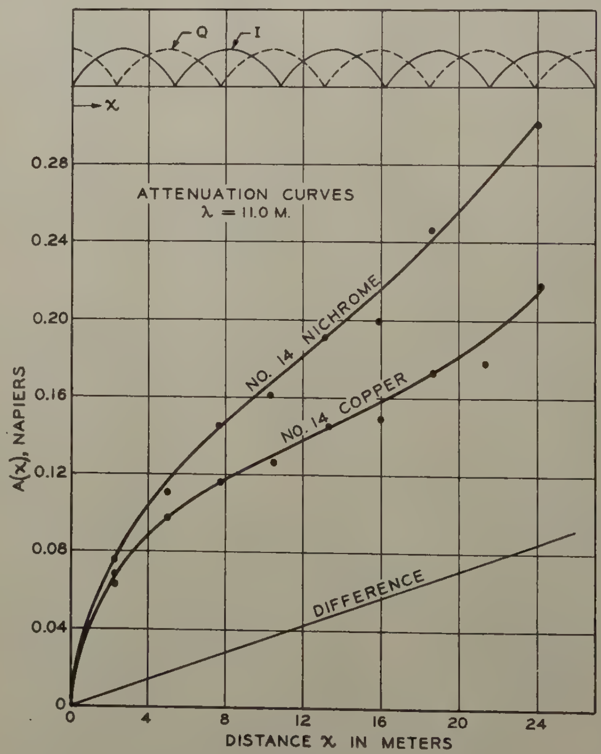

Fig. 6

the total attenuation measured at 11 meters wavelength appears in Fig. 6. The smooth curves, whose slopes are to be determined graphically, were drawn in among the scattered experimental points to conform

with the knowledge that the difference should increase linearly. The slope of this linear curve determines the characteristic impedance, knowing the difference in high-frequency resistance. The slope of the copper-wire curve (the high-frequency resistance is negligible) determines the radiation resistance at any point, knowing the characteristic impedance. The Nichrome-wire resistance was 3.56 ohms per meter at 11 meters wavelength, while the copper-wire resistance was 0.27 ohm per meter. Using these data the characteristic impedance is found to be 470 ohms which agrees well with calculation and other measurements. Radiation-resistance values so determined are plotted in Fig. 4 together with a curve calculated from (7).

III. Mathematical Analysis

Consider a cylindrical wire of radius a (Fig. 3) so energized that the electric current is parallel to the axis; then, the electric intensity E_x at the surface of the wire and parallel to it is

$$E_x = -i\omega\mu\Pi - \frac{dU}{dx}, \tag{15}$$

where the retarded electric scalar potential U and the retarded magnetic vector potential A are given[9] by (2).

Everywhere along the wire, except at the generator, the electric intensity E_x is also given by

$$E_x = ZI, \qquad Z = \frac{1}{2\pi a}\sqrt{\frac{i\omega\mu}{g}}, \tag{16}$$

where Z is the surface impedance of the wire and g is the conductivity. Substituting from (16) in (15), we have

$$\frac{dU}{dx} = -ZI - i\omega\mu\Pi. \tag{17}$$

We shall now carry out two successive approximations: First, we shall see what happens when the radius of the wire is approaching zero; then, starting from this approximation we shall compute certain correction terms. Consider the following factor in the integrand of (2)

$$\frac{e^{-i\beta r}}{r} = \frac{\cos\beta r}{r} - i\frac{\sin\beta r}{r}. \tag{18}$$

If a approaches zero, the first term approaches infinity in the immediate vicinity of $x'=x$ while the second term remains everywhere finite. Hence, from (2) we obtain the following asymptotic relations

$$\epsilon V(x) = A(x)q(x), \qquad \Pi(x) = A(x)I(x); \tag{19}$$

where

$$A(x) = \frac{1}{4\pi}\int_{-l}^{l}\frac{dx'}{r}. \tag{20}$$

[9] In the present case the vector potential is parallel to the wire.

Substituting from (19) in (17), we have

$$\frac{dq}{dx} = -\left[i\omega\mu\epsilon + \frac{\epsilon Z}{A(x)}\right]I - \frac{A'(x)}{A(x)}q. \tag{21}$$

Assuming that Z remains finite as $A(x)$ approaches infinity, we have

$$\frac{dq}{dx} = -i\omega\mu\epsilon I. \tag{22}$$

Next we calculate the effect of the second term in (18) on the values of the integrals in (2), assuming that I and q satisfy (22) and that the wire is energized at $x=0$. Thus we have[10]

$$\begin{aligned}
-i\int_{-l}^{l}\frac{\sin\beta r}{4\pi r}I(x')dx' &= \frac{1}{4\pi\omega\mu\epsilon}\int_{-l}^{l}\frac{\sin\beta r}{r}\frac{dq(x')}{dx'}dx' \\
&= \frac{1}{4\pi\mu\omega\epsilon}\left[q(l)\frac{\sin\beta r_1}{r_1} - q(+0)\frac{\sin\beta r_0}{r_0}\right. \\
&\quad + q(-0)\frac{\sin\beta r_0}{r_0} - q(-l)\frac{\sin\beta r_2}{r_2} \\
&\quad \left. - \int_{l}^{l} q(x')\frac{d}{dx'}\left(\frac{\sin\beta r}{r}\right)dx'\right],
\end{aligned} \tag{23}$$

where

$$r_0 = \sqrt{a^2+x^2}, \qquad r_1 = \sqrt{a^2+(l-x)^2}, \qquad r_2 = \sqrt{a^2+(l+x)^2}. \tag{24}$$

Similarly, we have

$$\begin{aligned}
\int_{-l}^{l}\frac{\sin\beta r}{4\pi r}q(x')dx' &= \frac{i}{\omega}\int_{-l}^{l}\frac{\sin\beta r}{4\pi r}\frac{dI(x')}{dx'}dx' \\
&= \frac{i}{\omega}I(x')\frac{\sin\beta r}{4\pi r}\Bigg|_{-l}^{l} \\
&\quad - \frac{i}{\omega}\int_{-l}^{l}I(x')\frac{d}{dx'}\left(\frac{\sin\beta r}{4\pi r}\right)dx'.
\end{aligned} \tag{25}$$

In this expression the first term vanishes if the current is equal to zero at the ends of the antenna.

Neglecting the last terms (the integrals) in (23) and (25), and substituting in (17), we obtain (neglecting also $A'(x)/A(x)$)

$$\begin{aligned}
\frac{dq}{dx} = -i\omega\mu\epsilon I - \frac{\epsilon ZI}{A(x)} - \frac{i}{4\pi A(x)}&\left[q(l)\frac{\sin\beta r_1}{r_1}\right. \\
&- q(+0)\frac{\sin\beta r_0}{r_0} + q(-0)\frac{\sin\beta r_0}{r_0} \\
&\left. - q(-l)\frac{\sin\beta r_2}{r_2}\right].
\end{aligned} \tag{26}$$

[10] If the wire is energized at $x=0$, $q(+0)$ is not equal to $q(-0)$.

Integrating (20), we have

$$A(x) = \frac{1}{4\pi}\log\frac{\sqrt{a^2+(l-x)^2}+(l-x)}{\sqrt{a^2+(l+x)^2}-(l+x)} \doteq \frac{1}{4\pi}\log\frac{4(l^2-x^2)}{a^2} \quad (27)$$

At the center of the wire and at the ends we have

$$A(0) = \frac{1}{2\pi}\log\frac{2l}{a}, \quad A(l) = A(-l) = \frac{1}{4\pi}\log\frac{4l}{a}. \quad (28)$$

The average value of $A(x)$ along the wire is

$$A(x)\Big|_{\text{av}} = \frac{1}{2\pi}\left(\log\frac{2l}{a} - 2 + 2\log 2\right). \quad (29)$$

This average value of $A(x)$ is related to the average capacitance C between two halves of the wire; thus we have very nearly

$$A(x)\Big|_{\text{av}} = \frac{\epsilon}{2C}. \quad (30)$$

Replacing $A(x)$ in (26) by its average value from (30), we have

$$\frac{dq}{dx} = -i\omega\mu\epsilon I - 2ZCI - \frac{iC}{2\pi\epsilon}\left[q(l)\frac{\sin\beta r_1}{r_1} - q(+0)\frac{\sin\beta r_0}{r_0} + q(-0)\frac{\sin\beta r_0}{r_0} - q(-l)\frac{\sin\beta r_2}{r_2}\right]. \quad (31)$$

This approximate equation has been obtained on the assumption that the wire is energized at the center; however, the same expression holds for any position of the generator, in which case x is measured from the generator.

For a centrally disposed generator we have in the first approximation

$$I(x) = I_0\sin\beta(l-x), \quad x>0, \qquad = I_0\sin\beta(l+x), \quad x<0, \quad (32)$$

where I_0 is the maximum amplitude of the current. Hence,

$$q(l) = -\frac{i\beta I_0}{\omega} = -i\sqrt{\mu\epsilon}\,I_0, \quad q(-l) = i\sqrt{\mu\epsilon}\,I_0, \qquad q(+0) = -q(-0) = -i\sqrt{\mu\epsilon}\,I_0\cos\beta l. \quad (33)$$

Substituting these values in (31), we obtain

$$\frac{dq}{dx} = -i\omega\mu\epsilon I - 2ZCI - 60CI_0\left(\frac{\sin\beta r_1}{r_1} - 2\frac{\sin\beta r_0}{r_0}\cos\beta l + \frac{\sin\beta r_2}{r_2}\right). \quad (34)$$

Since a is assumed to be small, we can write (34) as follows

$$\frac{dq}{dx} = -i\omega\mu\epsilon I - 2ZCI - 60CI_0\left[\frac{\sin\beta(l-x)}{l-x} - 2\frac{\sin\beta x}{x}\cos\beta l + \frac{\sin\beta(l+x)}{l+x}\right]. \quad (35)$$

It is quite obvious that the last term, representing approximately the effect of radiation on the electric charge and the electric current distribution in the antenna, differs in form from the second term $(-2ZCI)$, representing the effect of dissipation in the wire and the effect of the internal inductance of the wire. The latter term is always proportional to the current in the particular section of the antenna while the radiation term is not, as a rule. If, however, the length of the wire is equal to an odd number of half wavelengths,[11] then (35) becomes

$$\frac{dq}{dx} = -\left[i\omega\mu\epsilon + (2Z + 2R_{\text{rad}})C\right]I, \qquad R_{\text{rad}} = \frac{60l}{l^2-x^2}. \quad (36)$$

In this case, to the extent of our approximation, radiation is represented by a term similar to the dissipation term.

The approximate formula (7) for R_{rad} was also obtained by a different method in an earlier paper.[2] There a point was made of a curious paradox which seems to us important enough to bear a repetition. Assuming a sinusoidal current distribution ($I_0\sin\beta\bar{x}$) in an antenna whose length is equal to an integral number of half wavelengths, A. A. Pistolkors[12] obtains the following expression for the electric intensity parallel to the wire at its surface

$$-E_x = 30\left(\frac{1}{\bar{x}} + \frac{1}{2l-\bar{x}}\right)I_0\sin\beta\bar{x} + 30i\left[\frac{1}{\bar{x}} - \frac{1}{2l-\bar{x}}\right]I_0\cos\beta\bar{x}, \quad (37)$$

where $\bar{x}=l+x$ is the distance from an end of the wire. It is evident that the real part $-E_x/I(x)$ gives (7) for the radiation resistance. This cannot be regarded as anything more than a coincidence. If we were fortunate enough (or, perhaps, unfortunate) to know the *exact* current distribution in the antenna, then we should have found that E_x and, hence, $-E_x/I(x)$ are equal to 0 everywhere on the surface of the wire for the simple reason that $E_x=0$ is the boundary condition from which the correct current distribution must be determined. In an antenna energized at a point there is really no relation between R_{rad} and E_x.

[11] In fact, to any number of half wavelengths if the generator is located at a current antinode.

[12] A. A. Pistolkors, "The radiation resistance of beam antennas," Proc. I.R.E., vol. 17, pp. 562–579; March, 1929.

On the Pickup of Balanced Four-Wire Lines*

CHARLES W. HARRISON, JR.†, ASSOCIATE, I.R.E.

Summary—*It is demonstrated that for practical purposes the pickup of undesired energy by a balanced four-wire line when compared to the pickup of a balanced two-wire line of the same spacing is so small as to be considered negligible.*

SEVERAL methods are in general use for evaluating the power radiated from an antenna or transmission line. One of these methods consists in the integration of the normal component of the Poynting vector over the surface of a great sphere;[1–3] in the other method, the integration is carried out over the surface of the wires making up the radiating system.[4–6]

In the first method, a knowledge of the far-zone field is required. In the latter, one must have expressions for the electromagnetic field which are valid right up to the surface of the radiating wires. Naturally, this field is intrinsically more complicated than the field in the far zone.

There are certain inherent weaknesses in either approach. For a complicated array, the setting up of the radiation function and the carrying out of the integration in an application of the great sphere method is frequently very difficult. In such a case, the solution of a given problem often may be simplified by the use of the second method which implies a knowledge of the self and mutual impedances.

In setting up the radiation function, or the calculation of the self and mutual impedances, one is required to make some assumption regarding the current distribution. Otherwise, one must solve for the distribution using, for example, the methods of Hallén[7] or King.[8] The usual approach is to assume a current distribution of the form

$$I_z = I_0 \sin (L - \beta_0 |z|)/\sin L \tag{1}$$

for the sinusoidal case, and of the form

$$I_z = I_0 e^{-j\beta_0(l-z)} \tag{2}$$

for the traveling-wave case.

Here $L = \beta_0 l$

$$\beta_0 = \frac{2\pi}{\lambda}.$$

It may be well to say at this point that in the usual case, the assumption of the distribution given by (2) neglecting attenuation is as accurate as that assumed in (1).

It is known, however, that the condition imposed by (1) is fairly precise only in the physically impossible case of an infinitely thin conducting thread. Now in the reactive term of the general equation for the self-impedance, evaluated on the basis of a sine current distribution, the radius of the conductor appears. It follows, therefore, that under such conditions it is impossible to determine the reactance by the integration of the Poynting vector over the surface of a conductor of finite radius. In addition, one ordinarily assumes a perfect conductor in carrying out this method. The tangential electric field at the surface of the wires assuming a sinusoidal current distribution is not zero, which contradicts the boundary condition for a perfect conductor.

Happily, either of the methods gives the same results in so far as the evaluation of the power radiated from a line or antenna is concerned.

It has been the practice when calculating the power radiated from, or conversely, the pickup of, a transmission line, to neglect the effect of the terminations. Such a procedure involves not only neglecting the power radiated by the terminations, but also the mutual power. Some work is now being done on the radiation from lines, taking into account the terminations. For the present purposes, if one assumes an open-circuited transmission line a multiple of a half wave in length, with vanishing currents at the ends, a satisfactory equation for the radiation resistance can be obtained. Just how the radiation from the line as operated in practice compares with that so determined for the open-circuited case is not known. The nonresonant operation of a line is of great interest, but a determination of the power radiated from such a line should take into account the terminations. However, it remains to be demonstrated that the expressions for the radiation resistance of terminated two-wire transmission lines published to date are invalid. Accordingly, the case of a nonresonant balanced four-wire line, neglecting terminations, and the case of an open-circuited multiple half-wave balanced four-wire line are discussed here.

* Decimal classification: R116. Original manuscript received by the Institute, May 26, 1942.

† Cruft Laboratory, Harvard University, Cambridge, Massachusetts.

[1] Stuart Ballantine, "On the radiation resistance of a simple vertical antenna at wave lengths below the fundamental," Proc. I.R.E., vol. 12, pp. 823–832; December, 1924.

[2] S. A. Schelkunoff, "A general radiation formula," Proc. I.R.E., vol. 27, pp. 660–666; October, 1939.

[3] Ronold King, "The approximate representation of the distant field of linear radiators," Proc. I.R.E., vol. 29, pp. 458–464; August, 1941.

[4] A. A. Pistolkors, "The radiation resistance of beam antennas," Proc. I.R.E., vol. 17, pp. 562–579; March, 1929.

[5] Rudolf Bechmann, "On the calculation of radiation resistance of antennas and antenna combinations," Proc. I.R.E., vol. 19, pp. 1471–1480; August, 1931.

[6] P. S. Carter, "Circuit relations in radiating systems," Proc. I.R.E., vol. 20, pp. 1004–1041; June, 1932.

[7] E. Hallén, "Theoretical investigations into the transmitting and receiving qualities of antennas," *Nova Acta Upsaliensis*, ser. IV, vol. 11, pp. 1–44; November 11, 1938.

[8] L. V. King, "On the radiation field of a perfectly conducting base insulated cylindrical antenna over a perfectly conducting plane earth, and the calculation of radiation resistance and reactance," *Phil. Trans. Royal Soc.* (London), vol. 236, pp. 381–422; November 2, 1937.

An expression for the radiation resistance of a balanced line, the wires of which are fixed at the corners of a square, may be determined as follows: Refer to Fig. 1. Wires A and C and wires B and D are electrically paralleled. It can be readily shown, using standard

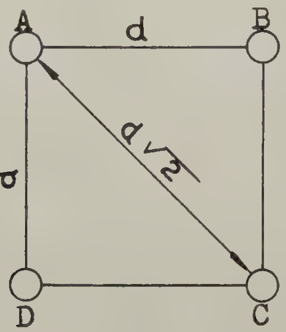

Fig. 1—Four-wire line.

electric circuit theory, that the radiation resistance expressed in ohms is

$$R = R_{11} - 2R_{AB} + R_{AC}. \tag{3}$$

Here R_{11} is the self-resistance of a conductor in ohms (similar conductors not displaced in length are assumed).

R_{AB} and R_{AC} are the mutual resistance in ohms between the conductors denoted by the subscripts.

For a line a multiple half wave in length, open-circuited at both ends,

$$R_{11} = 30 \overline{\text{Ci}}\, 2L \tag{4}$$

and

$$R_{(\text{mutual})} = 30[2 \text{ Ci } \beta_0 x - \text{Ci } \beta_0(y+l) - \text{Ci } \beta_0(y-l)] \tag{5}$$

where $y = \sqrt{l^2 + x^2}$

x = separation distance of the parallel wires.

$$\text{Ci }(z) = -\int_z^\infty \frac{\cos u}{u} du$$

$$\overline{\text{Ci}}\,(z) = \int_0^z \frac{1-\cos u}{u} du$$

Both (4) and (5) are based on the current distribution given by (1).

Using (4) and (5) in (3), and retaining the leading term after making the approximation $l \gg d$, one obtains

$$R_s \doteq 20\pi^4 \left(\frac{d}{\lambda}\right)^4. \tag{6}$$

Here R_s is the radiation resistance of a four-wire balanced line a multiple half wave in length, open-circuited at each end. d is the separation between constants, as shown in Fig. 1.

The self-resistance of an isolated nonresonant wire, as given in numerous places in the literature, is

$$R_{11} = 60\left(\overline{\text{Ci}}\, 2L - 1 + \frac{\sin 2L}{2L}\right) \text{ ohms} \tag{7}$$

and the corresponding equation for the mutual resistance worked out by the writer is

$$R_{(\text{mutual})} = 30\left[4 \text{ Ci } \beta_0 x - 2 \text{ Ci } \beta_0(y+l) - 2 \text{ Ci } \beta_0(y-l) - \frac{2 \sin \beta_0 x}{\beta_0 x} + \frac{\sin \beta_0(y-l)}{\beta_0 y} + \frac{\sin \beta_0(y+l)}{\beta_0 y}\right] \text{ ohms.} \tag{8}$$

Both (7) and (8) are based on the current distribution given by (2).

Using (7) and (8) in (3), and retaining the leading term after making the approximation $l \gg d$, one obtains

$$R_t \doteq 40\pi^4 \left(\frac{d}{\lambda}\right)^4. \tag{9}$$

Here R_t is the radiation resistance of a four-wire balanced transmission line on which a traveling wave system exists. The effect of the termination has not been taken into account.

The corresponding expressions published by Sterba and Feldman[9] for the two-wire line have been checked using the analysis given here. These expressions are

$$R_s \doteq 120\pi^2 \left(\frac{d}{\lambda}\right)^2 \tag{10}$$

and

$$R_t \doteq 160\pi^2 \left(\frac{d}{\lambda}\right)^2 \tag{11}$$

for the standing and traveling-wave cases, respectively.

It is apparent, upon a consideration of these equations, that the power radiated by a four-wire line for a given value of line current is extremely small compared to that radiated by a two-wire line of the same spacing.

Consequently, by reciprocation, the pickup of a four-wire line is very small compared to a similar two-wire line, and may be considered negligible for all practical purposes.

The writer believes that when the current is nonvanishing at the ends of a line, the actual power radiated will prove to be very much less than that indicated by the use of either (9) or (11). A very limited amount of experimental evidence substantiates this view.

[9] E. J. Sterba and C. B. Feldman, "Transmission lines," Proc. I.R.E., vol. 20, pp. 1163–1202; July, 1932.

A Graphical Method to Find the Optimal Operating Conditions of Triodes as Class C Telegraph Transmitters*

J. C. FROMMER†, NONMEMBER, I.R.E.

Summary—*The oscillation of a triode can be characterized by plate-supply voltage, swing of plate voltage, peak plate current, and angle of current flow. For medium-size transmitters it is economical to draw as much output power as consistent with the ratings of the tube. A graph has been plotted with the swing of plate voltage and peak plate current as co-ordinates showing the output and necessary bias if the plate-supply voltage is held at the rated value and the angle of plate-current flow is chosen to produce just the rated dissipation. Grid resistor, grid current, and grid dissipation can be established from another graph. All data are given in ratios applicable to any type of tube.*

I. Symbols

e_b = momentary value of plate voltage
i_b = momentary value of plate current
e_c = momentary value of grid voltage
i_c = momentary value of grid current
E_b = plate-supply voltage
I_b = average value of plate current
E_c = grid bias
I_c = average value of grid current
$e_{b\,\min}$ = plate voltage at its downward peak
$i_{b\,\max}$ = plate current at the moment of downward peak of plate voltage
$e_{c\,\max}$ = grid voltage at the moment of downward peak of plate voltage
$i_{c\,\max}$ = grid current at the moment of downward peak of plate voltage.
Θ = plate-current cutoff angle (half of the angle of plate current flow)
Θ_g = grid-current cutoff angle (half of the angle of grid-current flow)
P_1 = plate input power $= E_bI_b$
P_2 = plate output power
P_p = plate dissipation $= P_1 - P_2$
P_l = rated plate dissipation
P_g = grid dissipation
$P_{r(\mathrm{D.C.})}$ = power lost in the grid resistor due to direct current
$P_{r(\mathrm{A.C.})}$ = power lost in the grid resistor due to alternating current
I_l = unity of current $= P_l/E_b$
E_l = plate voltage at which, with the grid connected to the cathode, plate current is I_l
p = ratio of the output power and the rated plate dissipation $= P_2/P_l$
s = ratio of the plate swing and the plate-supply voltage $= 1-(e_{b\,\min}/E_b)$
μ = amplification factor
u = a parameter $= (\mu E_c - E_b)/E_l$
R_p = resistance reflected on the plate
R_g = resistance of the grid resistor
ω = angular frequency of the oscillation
t = time reckoned from the downward peak of the plate voltage
$F(\Theta)_k$ = symbol for the integral

$$\frac{1}{2}\int_{\omega t=-\Theta}^{+\Theta} (\cos\omega t - \cos\Theta)^k d\omega t$$

$G(\Theta)_k$ = symbol for the integral

$$\frac{1}{2}\int_{\omega t=-\Theta}^{+\Theta} \cos\omega t\left(\frac{\cos\omega t - \cos\Theta}{1-\cos\Theta}\right)^k d\omega t$$

II. Introduction

When setting the operating conditions of oscillators we have control of the plate-supply voltage, the drive voltage (degree of regeneration), the resistance reflected into the plate circuit, and the grid bias (grid resistor). According to these settings the swing of the plate voltage, the peak plate current, and the angle of current flow will assume different values. For each set of conditions the plate dissipation can be determined. With medium-size transmitting tubes, where the cost of power consumption is negligible compared with the first cost of the installation, it is generally desired to obtain the maximum possible output. This is reached with both the plate-supply voltage and the plate dissipation at their upper permissible (rated) value. Therefore, in the present paper the plate-supply voltage is taken to be the maximum permissible and all settings are eliminated in which the plate dissipation is above the permissible (because such conditions would damage the tube) or in which the plate dissipation is below the permissible maximum (because such conditions would not give the maximum possible output; for exceptions see the end of Section IV). The number of free variables can thus be reduced to two: the swing of the plate voltage and the peak plate current. For each set of these two variables we consider only that particular angle of plate-current flow at which the rated plate dissipation is just reached. For this particular angle parameters giving output and necessary bias are plotted on Fig. 1. This figure shows that the output increases with increased plate swing and with higher peak plate current, which stands to reason. Neither of these values, however, can be augmented

* Decimal classification: R133×R333. Original manuscript received by the Institute, March 27, 1942.
† Ajax Engineering Company, Chicago, Illinois.

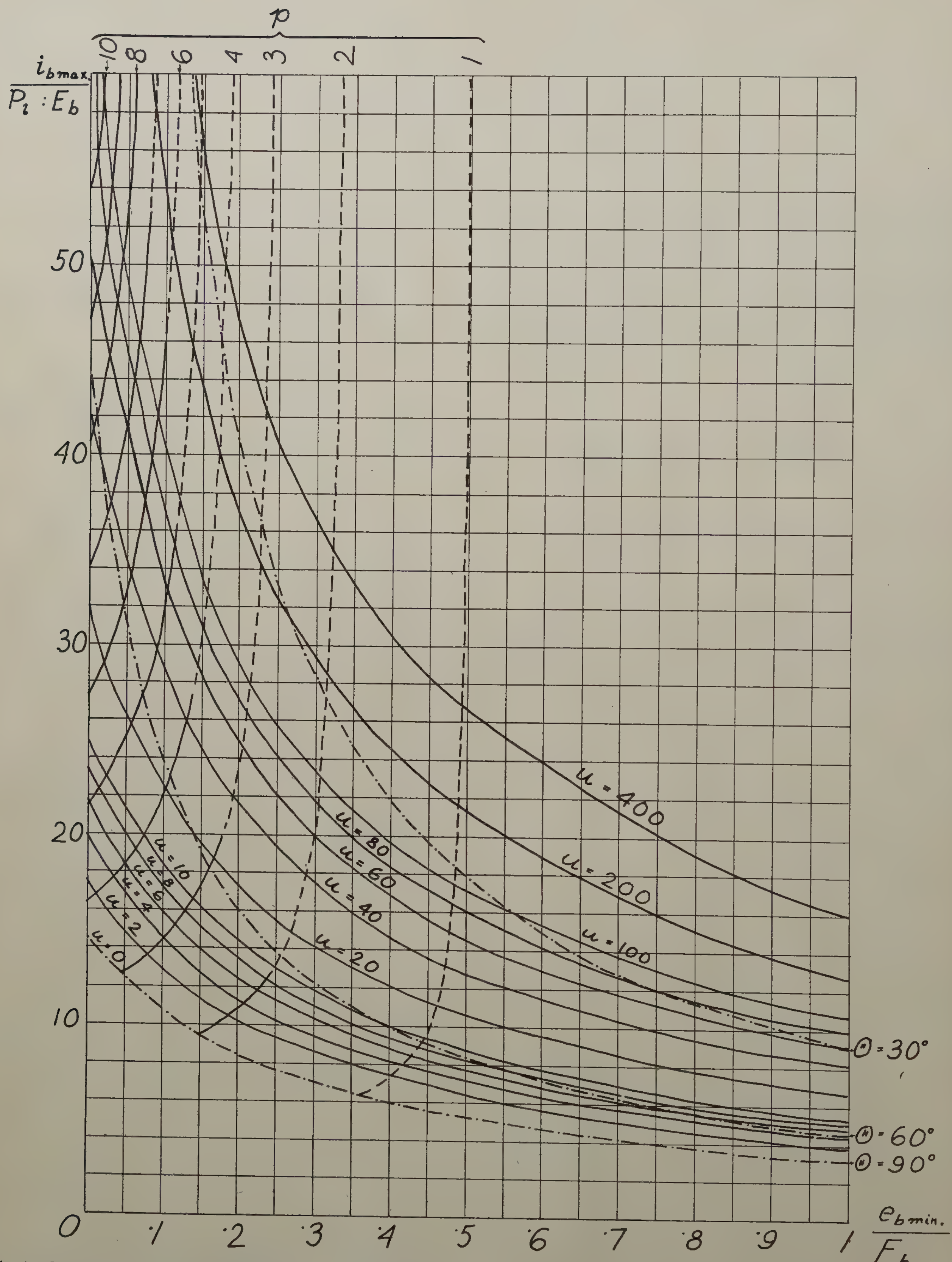

Fig. 1—Output obtainable as a function of plate-voltage swing and the peak value of plate current. To get some rated dissipation P_l, the plate-current cutoff angle has to be Θ, and with this angle the power output is pP_l. The parameter u serves to locate the necessary bias and with this the data of the grid circuit. Unity of the abscissa scale is the plate-supply voltage, and unity of the ordinate scale is the current obtained by dividing the rated plate dissipation by the plate-supply voltage.

without limit: the peak cathode current must never exceed the emission capacity of the cathode, the plate voltage swing must never assume a value at which the grid dissipation is excessive. We can easily trace these limits on the static characteristics of the tube. They are represented by two lines: one connecting points of equal cathode drain, another connecting the points at which the grid current starts to grow rapidly, say the points at which grid voltage equals plate voltage. The point of maximal output can be found at the upper left corner of the area so limited. The operating conditions pertaining to this point with an angle of current flow chosen to give the rated dissipation can be found from Figs. 1 and 2.

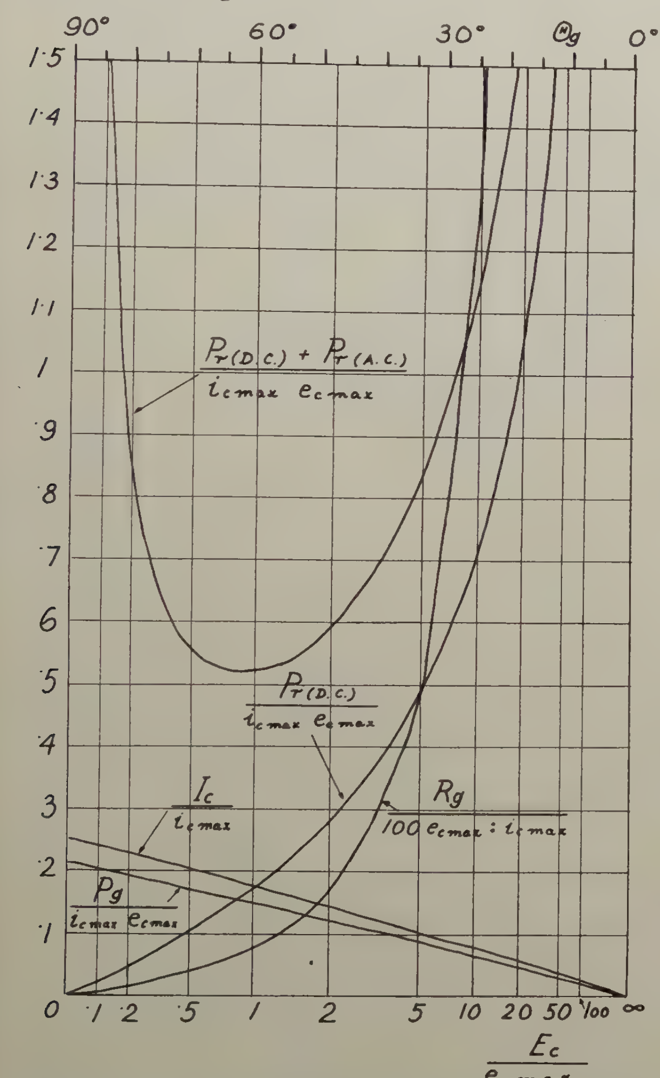

Fig. 2—Grid current, grid dissipation, necessary resistance of the grid resistor, and power consumed in this resistor. The abscissas are the ratio between bias and peak grid voltage. The ordinates are pure numbers, the functions being expressed with the peak grid voltage and peak grid current. These, in turn, can be found from the static characteristics of the tube if the plate-voltage swing and peak value of plate current are known.

III. Calculation of the Graphs

Fig. 3a represents an oscillator circuit. The plate of the tube is connected via one part of a tuned circuit to the positive terminal of the plate-voltage supply. Another section of the same tuned circuit is connected via a blocking condenser to the grid. The grid bias is generated by the grid current across the resistor R_g which is connected either directly or through a choke L_g to the grid. The load is generally inductively coupled, its effect can be represented by the resistance which it reflects into the plate circuit, R_p on the figure.

As a result of regeneration, there will arise an alternating voltage on the plate and on the grid. The time curves of these voltages and of the currents flowing to the plate and to the grid are represented on Figs. 3b and 3c. Because of the properties of tuned circuits these are in phase with each other and the voltages have a very low proportion of harmonics. These harmonics, as well as the phase shifting caused by electron transit time, are neglected in this paper.

Referring to Fig. 3, the instantaneous values of plate voltage and grid voltage are, respectively,

$$e_b = E_b(1 - s\cos\omega t) \tag{1}$$

$$e_c = -E_c + (E_c + e_{c\,\max})\cos\omega t. \tag{2}$$

As unity of current the value

$$I_l = \frac{P_l}{E_b} \tag{3}$$

is used, i.e., the continuous direct current which, at a plate voltage $e_b \equiv E_b$ would just cause the rated plate dissipation. The voltage E_l is defined as the plate voltage at which, with the grid connected to the cathode, a plate current I_l would be drawn from the tube.

If the amplification factor of the tube is μ, the plate current is, according to the space-charge law,

$$i_b = I_l\left(\frac{e_b + \mu e_c}{E_l}\right)^\alpha. \tag{4}$$

Because of grid current, actual conditions are best represented with an exponent α being lower than the theoretical 3/2.

Substituting (1) and (2) into (4),

$$\frac{i_b}{I_l} = \left(\frac{E_b - \mu E_c}{E_l} + \frac{\mu E_c + \mu e_{c\,\max} - sE_b}{E_l}\cos\omega t\right)^\alpha. \tag{5}$$

Denote

$$\frac{\mu E_c - E_b}{E_l} = u. \tag{6}$$

Substituting (6) into (5) and remembering that i_b is 0 when $\omega t = \Theta$ (cutoff angle of plate-current flow), write

$$\frac{i_b}{I_l} = \left(-u + \frac{u}{\cos\Theta}\cos\omega t\right)^\alpha. \tag{7}$$

The peak plate current $i_{b\,\max}$ is reached at $\omega t = 0$.

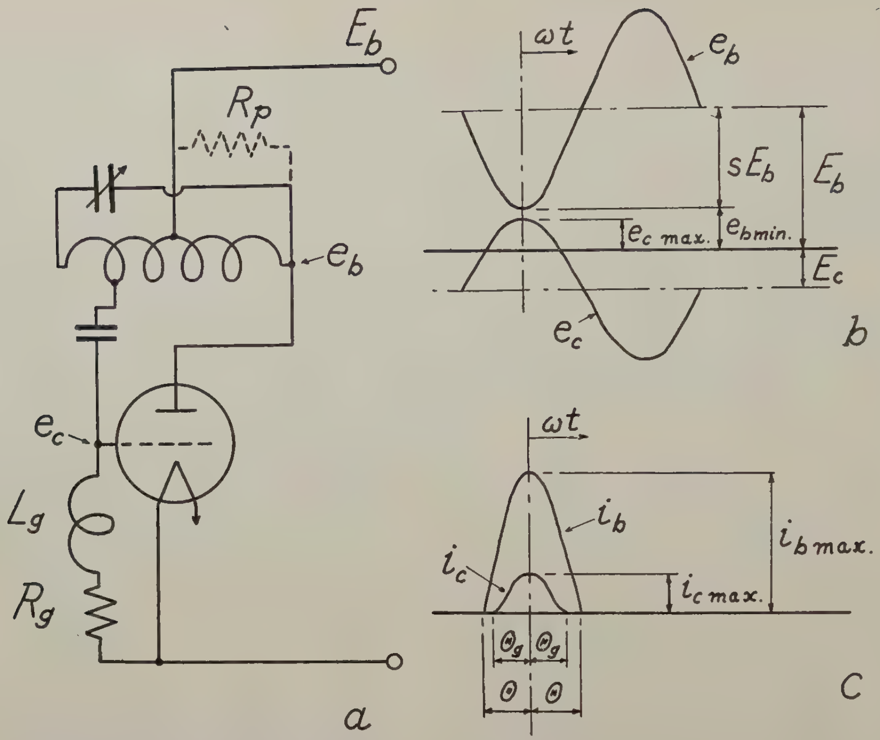

Fig. 3—Fundamentals. a. Schematic of a self-excited oscillator circuit. b. Time curves of plate voltage and grid voltage. c. Time curve of plate current and grid current.

Hence,

$$\frac{i_{b\,\max}}{I_l} = \left(-u + \frac{u}{\cos\Theta}\right)^{\alpha}. \tag{8}$$

Dividing (7) by (8),

$$\frac{i_b}{i_{b\,\max}} = \left(\frac{\cos\omega t - \cos\Theta}{1 - \cos\Theta}\right)^{\alpha}. \tag{9}$$

The mean value of plate current is

$$I_b = \frac{1}{2\pi}\int_{-\Theta}^{+\Theta} i_b d\omega t. \tag{10}$$

With (9),

$$I_b = \frac{1}{2\pi}\int_{-\Theta}^{+\Theta} i_{b\,\max}\left(\frac{\cos\omega t - \cos\Theta}{1 - \cos\Theta}\right)^{\alpha} d\omega t. \tag{11}$$

With the symbol,

$$F(\Theta)_\alpha = \frac{1}{2}\int_{-\Theta}^{+\Theta}\left(\frac{\cos\omega t - \cos\Theta}{1 - \cos\Theta}\right)^{\alpha} d\omega t. \tag{12}$$

$$I_b = \frac{1}{\pi} i_{b\,\max} F(\Theta)_\alpha. \tag{13}$$

The input power is

$$P_1 = E_b I_b = E_b \frac{1}{\pi} i_{b\,\max} F(\Theta)_\alpha. \tag{14}$$

The output power is

$$P_2 = \frac{1}{2\pi}\int_{-\Theta}^{+\Theta} (E_b - e_b) i_b d\omega t. \tag{15}$$

Substituting (1) and (9),

$$P_2 = \frac{1}{2\pi}\int_{-\Theta}^{+\Theta} E_b s \cos\omega t\, i_{b\,\max}\left(\frac{\cos\omega t - \cos\Theta}{1 - \cos\Theta}\right)^{\alpha} d\omega t. \tag{16}$$

By denoting

$$\frac{1}{2}\int_{-\Theta}^{+\Theta} \cos\omega t\left(\frac{\cos\omega t - \cos\Theta}{1 - \cos\Theta}\right)^{\alpha} d\omega t = G(\Theta)_\alpha, \tag{17}$$

(16) can be written

$$P_2 = \frac{1}{\pi} s E_b i_{b\,\max} G(\Theta)_\alpha. \tag{18}$$

With (13), (18) can be written

$$P_2 = s E_b I_b \frac{G(\Theta)_\alpha}{F(\Theta)_\alpha}. \tag{19}$$

With (14) and (19) the plate dissipation is

$$P_p = P_1 - P_2 = E_b I_b \left(1 - s\frac{G(\Theta)_\alpha}{F(\Theta)_\alpha}\right). \tag{20}$$

Now, the graph has to be drawn for the condition that the plate dissipation equals its rated value:

$$P_p = P_l. \tag{21}$$

From (19), (20), (21) the proportion between the output and the plate dissipation is

$$p = \frac{P_2}{P_l} = \frac{s\dfrac{G(\Theta)_\alpha}{F(\Theta)_\alpha}}{1 - s\dfrac{G(\Theta)_\alpha}{F(\Theta)_\alpha}} \tag{22}$$

from whence

$$s = \frac{p}{1+p} \frac{F(\Theta)_\alpha}{G(\Theta)_\alpha}. \tag{23}$$

From (3) and (13)

$$\frac{i_{b\,\max}}{I_l} = \frac{\pi}{F(\Theta)_\alpha} \frac{E_b I_b}{P_l}. \tag{24}$$

This can be written with (20), (21), and (22)

$$\frac{i_{b\,\max}}{I_l} = \frac{\pi}{F(\Theta)_\alpha}(1+p). \tag{25}$$

From (6)

$$E_c = \frac{uE_l + E_b}{\mu}. \tag{26}$$

To draw Fig. 1, calculate the numerical values of $F(\Theta)_\alpha$ and $G(\Theta)_\alpha$ for different values of Θ between 0 and 90 degrees. Now, with Θ as a parameter, draw the p lines for the different values of p, using (23) for the abscissas and (25) for the ordinates. Connect the points pertaining to the same value of Θ. Draw the lines for the different values of u with Θ as a parameter using (8) for the ordinates and finding the abscissas by intersection with the corresponding Θ curve. The Θ curves serve only for the construction of the u curves. To simplify the figure, only a few of these lines have been left in the graph. The abscissas are marked with $e_{b\,\min}/E_b = 1-s$.

To reckon the curves of Fig. 2, denote the cutoff angle of grid current flow by Θ_g and remember that grid current starts and stops when $e_c = 0$. Hence

$$(E_c + e_{c\,\max}) \cos \Theta_g = E_c \tag{27}$$

or

$$\frac{E_c}{e_{c\,\max}} = \frac{\cos \Theta_g}{1 - \cos \Theta_g}. \tag{28}$$

Now, from (2) and (27):

$$e_c = E_c \frac{\cos \omega t - \cos \Theta_g}{\cos \Theta_g} \tag{29}$$

from whence

$$\frac{e_c}{e_{c\,\max}} = \frac{\cos \omega t - \cos \Theta_g}{1 - \cos \Theta_g}. \tag{30}$$

Assume that the grid current is proportional to the βth power of the grid voltage:

$$\frac{i_c}{i_{c\,\max}} = \left(\frac{\cos \omega t - \cos \Theta_g}{1 - \cos \Theta_g}\right)^\beta, \tag{31}$$

from whence

$$I_c = \frac{1}{2\pi}\int_{-\theta_g}^{+\theta_g} i_c d\omega t$$

$$= \frac{1}{2\pi}\int_{-\theta_g}^{+\theta_g} i_{c\,\max}\left(\frac{\cos \omega t - \cos \Theta_g}{1 - \cos \Theta_g}\right)^\beta d\omega t. \tag{32}$$

With the symbol given in (12),

$$I_c = \frac{1}{\pi} F(\Theta_g)_\beta i_{c\,\max}. \tag{33}$$

The power consumption on the grid is

$$P_g = \frac{1}{2\pi}\int_{-\theta_g}^{+\theta_g} e_c i_c d\omega t \tag{34}$$

with (30), (31), and the symbol given in (12),

$$P_g = \frac{1}{\pi} F(\Theta_g)_{\beta+1} e_{c\,\max}\, i_{c\,\max}. \tag{35}$$

The grid resistor must have the value

$$R_g = \frac{E_c}{I_c} = \frac{e_{c\,\max}}{i_{c\,\max}} \frac{\cos \Theta_g}{1 - \cos \Theta_g} \frac{\pi}{F(\Theta_g)_\beta}, \tag{36}$$

E_c and I_c being substituted from (28) and (33).

If alternating current is withheld from the grid by the choke coil L_g, the power lost in this resistor is

$$P_{r(\mathrm{D.C.})} = E_c I_c = e_{c\,\max}\, i_{c\,\max} \frac{\cos \Theta_g}{1 - \cos \Theta_g} \frac{F(\Theta_g)_\beta}{\pi}. \tag{37}$$

If no choke is used, the grid resistor will carry an alternating current corresponding to the alternating voltage on the grid. The peak value of this alternating voltage is $E_c + e_{c\,\max}$. The additional power consumption is, therefore,

$$P_{r(\mathrm{A.C.})} = \frac{(E_c + e_{c\,\max})^2}{2R_g} \tag{38}$$

which with (27) and (36) is

$$P_{r(\mathrm{A.C.})} = \left(\frac{E_c}{\cos \Theta_g}\right)^2 \frac{I_c}{2E_c} = \frac{E_c I_c}{2(\cos \Theta_g)^2}. \tag{39}$$

From the addition of (37) and (39), the full power lost on the grid resistor in this case is

$$P_{r(\mathrm{D.C.})} + P_{r(\mathrm{A.C.})}$$

$$= e_{c\,\max}\, i_{c\,\max} \frac{\cos \Theta_g F(\Theta_g)_\beta}{(1 - \cos \Theta_g)\pi}\left(1 + \frac{1}{2(\cos \Theta_g)^2}\right). \tag{40}$$

From (33), (35), (36), (37), and (40)

$$\frac{I_c}{i_{c\,\max}}, \quad \frac{P_g}{i_{c\,\max}\, e_{c\,\max}}, \quad \frac{R_g}{100 e_{c\,\max} : i_{c\,\max}},$$

$$\frac{P_{r(\mathrm{D.C.})}}{i_{c\,\max}\, e_{c\,\max}}, \quad \frac{P_{r(\mathrm{D.C.})} + P_{r(\mathrm{A.C.})}}{i_{c\,\max}\, e_{c\,\max}}$$

are reckoned for various values of Θ_g and plotted on Fig. 2. The ordinates are marked with the ratio $E_c/e_{c\,\max}$ as reckoned from (28).

[1] If secondary emission takes place on the grid, the dissipation is higher.

We set the exponent $\alpha=1$, the exponent[2] $\beta=2$. With these values the integrals can be obtained in an elementary way.

IV. Setting of the Operating Conditions for a Given Type of Tube

To use the graphs for any individual type of tubes follow this procedure.

1. Divide the rated plate dissipation with the rated plate-supply voltage to obtain

$$I_l = \frac{P_l}{E_b}. \tag{3}$$

2. Find on the static characteristics of the tube the plate voltage E_l at which, with the grid voltage $e_c=0$, the plate current is I_l.

3. Set the amount of permissible peak cathode current. If not specified by the manufacturer take for each watt of heating power 8 milliamperes for pure-tungsten cathodes, 30 milliamperes for thoriated cathodes, and 100 milliamperes for oxide-coated cathodes.

4. Find along the $e_c=e_b$ line of the static characteristics the point at which the plate current plus twice the grid current[3] equals the permissible peak cathode current.

5. Divide the plate voltage pertaining to this point by E_b to obtain

$$\frac{e_{b\,\min}}{E_b}$$

and divide the plate current pertaining to this point by $I_l=P_l/E_b$ to obtain

$$\frac{i_{b\,\max}}{P_l:E_b}.$$

These are the co-ordinates in Fig. 1 of this point of operation.

6. Find on Fig. 1 the values of p and u pertaining to this point of operation and calculate the necessary bias

$$E_c = \frac{uE_l + E_b}{\mu} \tag{26}$$

and the output to be obtained

$$P_2 = pP_l. \tag{22}$$

7. Find on the static characteristics of the tube the grid voltage and the grid current pertaining to the point of operation. Form the quotient $E_c/e_{c\,\max}$. Find the necessary grid resistor, the grid dissipation, the mean grid current and the power consumed in the resistor with the coefficients on Fig. 2.

[2] W. G. Wagener, "Performance of transmitting tubes," Proc. I.R.E., vol. 25, pp. 47–77, January, 1937. See pages 51 and 60.

[3] The current density is higher near the grid wires. If the grid wires are close wound the factor 2 can be reduced.

If the grid dissipation is found to be too high, choose a new point of operation slightly to the right of the earlier one.

8. The resistance which has to be reflected to the plate is

$$R_p = \frac{(sE_b)^2}{2P_2} = \frac{s^2}{2p}\,\frac{E_b^2}{P_l}.$$

9. The peak value of necessary driving voltage is $e_{c\,\max}+E_c$. If the tube is self-excited, as on Fig. 3, the necessary factor of regeneration is the ratio between the peak of the grid voltage and the peak of the plate-voltage swings:

$$\frac{E_c + e_{c\,\max}}{sE_b}.$$

A self-excited tube draws the driving power from the plate circuit; accordingly, for self-excited tubes, grid dissipation and power lost on the grid resistor have to be deducted from the output found on Fig. 1.

Numerical Example.

A triode (Taylor T 40) has a thoriated cathode for 7.5 volts, 2.5 amperes. Its amplification factor is $\mu=25$. Its continuous commercial service ratings are $E_b=1250$ volts, $P_l=40$ watts.

1. $I_l = \dfrac{P_l}{E_b} = \dfrac{40}{1250} = 32$ milliamperes.

2. On the static characteristics the $e_c=0$ line assumes $i_b=32$ milliamperes at $e_b=600$ volts. Thus, $E_l=600$ volts.

3. Allow a peak cathode current of 7.5 volts$\times$2.5 amperes$\times$30 milliamperes per watt$=$563 milliamperes.

4. On the static characteristics of the tube we find that with $e_b=e_c=130$ volts, $i_b=400$ milliamperes, and $i_c=85$ milliamperes. $400+2\times85=570$; thus we choose this point as peak of plate swing (point of operation) and write $e_{b\min}=130$ volts, $e_{c\max}=130$ volts, $i_{b\max}=400$ milliamperes, and $i_{c\max}=85$ milliamperes.

5. $\dfrac{e_{b\,\min}}{E_b} = \dfrac{130}{1250} = 0.104$

$$\frac{i_{b\,\max}}{P_l:E_b} = \frac{400}{32} = 12.5$$

6. On Fig. 1 we find that at the point with these co-ordinates $p=2.7$, $u=1.7$. Thus the grid bias has to be

$$E_c = \frac{uE_l + E_b}{\mu} = \frac{1.7\times600+1250}{25} = 91 \text{ volts.}$$

The power output is $P_2=pP_l=2.7\times40=108$ watts.

7. Write $i_{c\max}\,e_{c\max}=85$ milliamperes$\times$130 volts$=11$ watts; $e_{c\max}:i_{c\max}=130$ volts$:85$ milliamperes$=1530$ ohms.

$$\frac{E_c}{e_{c\,\max}} = \frac{91}{130} = 0.7$$

On Fig. 2 we find at this ordinate the grid dissipation $P_g = 0.16 \times i_{c\max} e_{c\max} = 0.16 \times 11 = 1.76$ watts the main grid current: $I_c = 0.2\ i_{c\max} = 0.2 \times 85 = 17$ milliamperes the necessary grid resistor $R_g = 0.04 \times 100 \times e_{c\max} : i_{c\max} = 0.04 \times 100 \times 1530 = 6100$ ohms. As the curve cannot be read properly at this low value take the more exact value

$$\frac{E_c}{I_c} = \frac{91 \text{ volts}}{17 \text{ milliamperes}} = 5350 \text{ ohms.}$$

The power lost on this resistor if direct current only is allowed to pass it $P_{r(\text{D.C.})} = 0.13\ i_{c\max} e_{c\max} = 0.13 = 11 = 1.43$ watts. The power lost on this resistor if it is connected to grid

$$P_{r(\text{D.C.})} + P_{r(\text{A.C.})} = 0.52 i_{c\,\max}\, e_{c\,\max} = 0.52 \times 11 = 5.7 \text{ watts}$$

8. The resistance reflected on the plate should be

$$R_p = \frac{s^2}{2p} \frac{E_b^2}{P_l} = \frac{(1 - 0.104)^2}{2 \times 2.7} \frac{1250^2}{40} = 5800 \text{ ohms.}$$

9. The necessary proportion of feedback is

$$\frac{E_c + e_{c\,\max}}{sE_b} = \frac{130 + 91}{(1 - 0.104) \times 1250} = 0.197.$$

If a tube is poorly designed or designed mainly for other services, and the capacity of emission of the cathode does not match the capacity of dissipation of the plate, the following irregularities will be noticed:

If the cathode is too weak the point of operation will fall below the line $u=0$. This means that the rated dissipation would not be reached even[4] with $\Theta = 90$ degrees. In such a case we still take $u=0$, but we note that the dissipation is below the rated in the proportion of the height of the actual point of operation to the height of the point of the $u=0$ line vertically above it. The power output will be the output pertaining to this latter point reduced in the same proportion.

With an overdimensioned cathode the point of operation will fall into the region where the p curves are drawn with dotted lines. In this case we will generally find on the $e_c = e_b$ line of the static characteristics a point lower than that found with the limit of cathode current, giving more output than that first. To find this point, draw the $e_c = e_b$ curve of the tube (with its co-ordinates expressed in terms of E_b and I_l) on Fig. 1 and find the point at which this line touches the (interpolated) line of greatest output. This new point of operation will give more output with a smaller peak cathode current.

The method described here has been used to set the operating conditions of a full line of transmitting tubes. The experimental results always corresponded perfectly to the predicted values except that the adjustment for regeneration had sometimes to be slightly different from that calculated. We attributed this to stray coupling between other parts of the plate circuit and the grid circuit. Life tests with our settings gave very satisfactory results.

[4] Theoretically, with Θ up to about 120 degrees, a slightly higher output could be gained, but practically this is not recommended.

CORRECTIONS

Discussion on
"The Distribution of Amplitude with Time in Fluctuation Noise"*

VERNON D. LANDON

In the equations of the above discussion by K. A. Norton and Vernon D. Landon, errors occurred in the publication of certain exponents, which were originally submitted in correct form by the authors. The right-hand sides of the following equations should have appeared as given below.

$$\frac{2}{n} \exp\left(-V^2/n\right) V dV \tag{1a}$$

$$100 \exp\left(-V^2/n\right) \tag{2a}$$

$$\frac{2}{E_1^2 + E_2^2 + \cdots + E_n^2} \cdot \exp\left(-V^2/(E_1^2 + E_2^2 + \cdots + E_n^2)\right) V dV \tag{1b}$$

* PROC. I.R.E., vol. 30, pp. 425–429; September, 1942.

$$100 \exp\left(-V^2/(E_1^2 + E_2^2 + \cdots + E_n^2)\right) \tag{2b}$$

$$\frac{2}{E^2} \exp\left(-V^2/E^2\right) V dV \tag{1c}$$

$$100 \exp\left(-V^2/E^2\right) \tag{2c}$$

$$\frac{2V}{E^2} \exp\left(-V^2/E^2\right) \tag{17}$$

$$\frac{2}{\pi E^2} \int_{-\infty}^{+\infty} \frac{V}{\sqrt{V^2 - v^2}} \exp\left(-V^2/E^2\right) dV \tag{19}$$

$$\frac{1}{E\sqrt{\pi}} \exp\left(-v^2/E^2\right) \tag{20}$$

$$\frac{1}{E\sqrt{\pi}} \int_{-\infty}^{+\infty} v^2 \exp\left(-v^2/E^2\right) dv = \frac{E^2}{2} \tag{21}$$

Books

Radiotron Designer's Handbook (third edition), edited by F. Langford Smith.

Published by the Wireless Press for the Amalgamated Wireless Valve Company, Sydney, Australia. Wholly reproduced in the United States by lithograph process by the RCA under the direction of the RCA Manufacturing company, Harrison, N. J. 352+iv pages+8-page index. 268 illustrations. $5\frac{1}{2} \times 8\frac{1}{2}$ inches. Price, $1.00

"This handbook has been prepared expressly for the radio set designer, but will be found invaluable to all radio engineers, experimenters, and service mechanics. The information is arranged so that all those interested may derive some knowledge with the minimum of effort in searching"—Foreword. It is recommended to all radio workers as a compact collection of information on radio apparatus; the principles governing its design, the performance of many practical arrangements, and the formulas and tables which are most helpful to the designer.

The range of subjects is limited to the scope of radio broadcast receivers, and is unusually complete within this scope. The emphasis is on laborsaving, so the explanations are brief and there is a generous supply of useful charts and formulas for all purposes. On every subject, there is a bibliography of further information, and these references are well chosen.

HAROLD A. WHEELER
Hazeltine Service Corporation
Little Neck, L. I., N. Y.

Standard Handbook for Electrical Engineers (seventh edition), edited by Archer E. Knowlton.

Published by McGraw-Hill Book Company, Inc., 330 W. 42 St., New York, N.Y. Revised and enlarged, August, 1941. 2278+xi pages+25-page index. 1757 figures. $6\frac{1}{2} \times 9 \times 2\frac{1}{2}$ inches. Price, $8.00.

This edition follows the sixth edition after a lapse of eight years. The first noticeable change is the size. The page size of previous editions, based upon the original intention of a pocket or "hand" book, has been abandoned. The printed area of the page has been increased over sixty per cent. The number of pages has been reduced and the size type has been increased but the sum total remains an effective increase in content. This volume is much easier to read and to handle than the previous edition.

The material in the book follows the general plan of that in previous editions. Some reorganizing has been done so as to reduce the number of sections from twenty-eight to twenty-six. More emphasis has been put upon those parts in which there has been an increase in technology since the last edition. The three sections covering Wire Communication, Radio and Carrier Communication, and Electronics encompass the same number of pages in this volume as in the previous edition giving a proportionate increase.

Some sections have been merely revised and brought up to date, while others have been entirely rewritten. In the revised sections, new methods of presentation are to be found. Throughout, antiquated material has been dropped, and new material substituted.

The index has been enlarged to include mention of a subject when treated incidentally as part of other subject matter.

This book is valuable to the radio, electronic, or wire communication engineer, not for the treatment of his particular subject but for the basic information on closely allied engineering art of which he occasionally finds himself in need.

R. A. HEISING
Bell Telephone Laboratories, Inc.
New York, N. Y.

Contributors

W. G. Cady

W. G. Cady (A'24–F'27) was born on December 10, 1874, at Providence, Rhode Island. He received the Ph.B. degree in 1895 and the M.A. degree in 1896 from Brown University, the Ph.D. degree from the University of Berlin in 1900, and the D.Sc. degree in 1938 from Brown University. From 1895 to 1897, he was an instructor in mathematics at Brown University, and from 1900 to 1902 he was a magnetic observer with the United States Coast and Geodetic Survey. He became an instructor in physics at Wesleyan University in 1902; associate professor in 1904; and since 1907 has been a professor. He was a member of the Board of Direction of the Institute of Radio Engineers in 1928 and President in 1932. Dr. Cady received the Morris Liebmann Memorial Prize from the Institute of Radio Engineers in 1928 and the Duddell Medal from the Physical Society of London in 1937. He was a member of the Division of National Sciences of the National Research Council from 1935 to 1938.

❖

Carl B. Feldman (A'26) was born at St. Peter, Minnesota, on March 26, 1902. He received the B.S. degree in 1926 and the M.S. degree in 1928 from the University of Minnesota. Since 1928 Mr. Feldman has been with the Bell Telephone Laboratories.

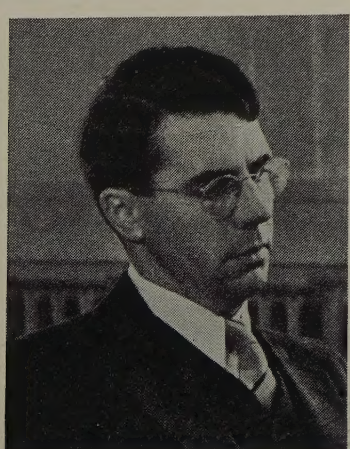

Carl B. Feldman

❖

J. C. Frommer

Joseph Charles Frommer was born at Budapest in 1904. He received the degree of mechanical engineering from the Hungarian Technical University in 1925 and did research work there the following year. From 1926 to 1927 Mr. Frommer worked in the Liancourt (France) plant of agricultural tractors of the Austin automobile works, and from 1928 to 1929 in a textile mill in Budapest. From 1929 to 1939 he was a member of the research laboratory of the United Incandescent Lamp and Electric Co. (TUNGSRAM works), Ujpest, Hungary, doing research work in connection with the production of photocells, vacuum tubes, incandescent lamps, design of valve circuits, and the setting of operating ratings. During 1940–1941 he was employed at the McKay-Massey-Harris Harvester works, Sunshine, Australia, and during 1941–1942 he did development work at the Beck-Lee Corporation in Chicago. He is now in charge of the research department of the Ajax Engineering Company in Chicago.

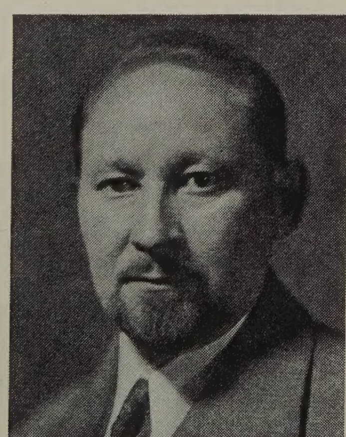

S. A. Schelkunoff

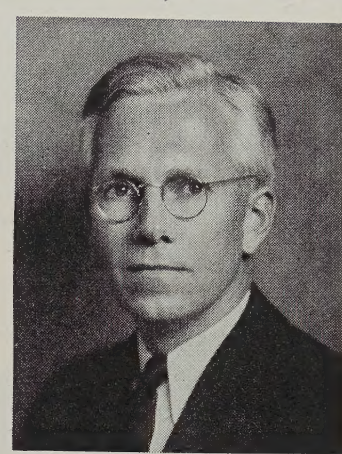

Karl S. Van Dyke

❖

For a biographical sketch of C. W. Harrison, Jr., see the Proceedings for May, 1942; for Jesse B. Sherman, see the Proceedings for January, 1942.

❖

S. A. Schelkunoff (A'40) received the B.A. and M.A. degrees in mathematics from the State College of Washington in 1923, and the Ph.D. degree in mathematics from Columbia University in 1928. He was in the engineering department of the Western Electric Company from 1923 to 1925; the Bell Telephone Laboratories from 1925 to 1926; the department of mathematics of the State College of Washington, 1926 to 1929; and Bell Telephone Laboratories, 1929 to date. Dr. Schelkunoff has been engaged in mathematical research, especially in the field of electromagnetic theory.

❖

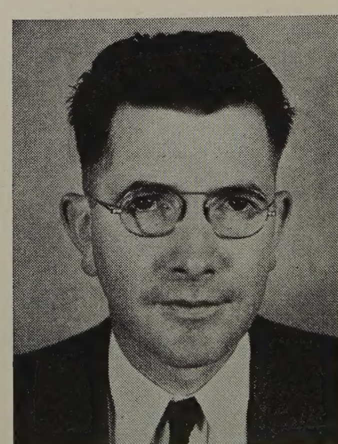

Lawrence A. Ware

Karl S. Van Dyke (A'15–M'26) was born at Brooklyn, New York, on December 8, 1892. He received the B.S. degree in 1916 and the M.S. degree in 1917 from Wesleyan University, and the Ph.D. degree in 1921 from the University of Chicago. From 1916 to 1917 Dr. Van Dyke was an assistant in physics at Wesleyan University; 1917 to 1919 in the general engineering department of the American Telephone and Telegraph Company; 1919 to 1921, assistant in physics at the University of Chicago; 1921 to 1925, an assistant professor of physics at Wesleyan University; 1925 to 1928, associate professor; and 1928 to date, professor. He is a Fellow of the American Association for the Advancement of Science, and a Member of the American Physical Society, the Acoustical Society of America, and Sigma Xi.

Lawrence A. Ware (A'41) was born at Bonaparte, Iowa, on May 21, 1901. He received the B.E. degree in electrical engineering in 1926, the M.S. degree in physics in 1927, the Ph.D. degree in physics in 1930, and the E.E. degree in 1935, all from the University of Iowa. From 1929 to 1933 Dr. Ware was a transmission engineer with the Bell Telephone Laboratories; from 1935 to 1937 he was assistant professor of physics at Montana State College; and since 1937 he has been assistant professor of electrical engineering at the University of Iowa. He is a member of the American Institute of Electrical Engineers, the American Physical Society, Eta Kappa Nu, Sigma Xi, and Tau Beta Pi.